INTERNATIONAL JOURNAL FOR NUMERICAL METHODS IN FLUIDS
Int. J. Numer. Meth. Fluids 0000; **00**:1–28
Published online in Wiley InterScience (www.interscience.wiley.com). DOI: 10.1002/fld

A Roe Scheme for a Compressible Six-Equation Two-Fluid Model

Alexandre Morin[1*], Tore Flåtten[2] and Svend Tollak Munkejord[2]

[1] *Department of Energy and Process Engineering, Norwegian University of Science and Technology (NTNU), Kolbjørn Hejes vei 1B, NO-7491 Trondheim, Norway.*

[2] *SINTEF Energy Research, P.O. Box 4761 Sluppen, NO-7465 Trondheim, Norway*

SUMMARY

We derive a partially analytical Roe scheme with wave limiters for the compressible six-equation two-fluid model. Specifically, we derive the Roe averages for the relevant variables. First, the fluxes are split into a convective and a pressure part. Then, independent Roe conditions are stated for these two parts. These conditions are successively reduced while defining acceptable Roe averages. For the convective part, all the averages are analytical. For the pressure part, most of the averages are analytical, while the remaining averages are dependent on the thermodynamic equation of state. This gives a large flexibility to the scheme with respect to the choice of equation of state. Furthermore, this model contains non-conservative terms. They are a challenge to handle right, and it is not the object of this paper to discuss this issue. However, the Roe averages presented in this paper are fully independent from how those terms are handled, which makes this framework compatible with any treatment of non-conservative terms. Finally, we point out that the eigenspace of this model may collapse, making the Roe scheme inapplicable. This is called resonance. We propose a fix to handle this particular case. Numerical tests show that the scheme performs well.

Received ...

KEY WORDS: Two-fluid model; Roe scheme; Resonance

1. INTRODUCTION

The two-fluid model is an option to simulate one-dimensional two-phase flows in pipelines [1, 2, 3, 4]. It is extensively used, particularly in the petroleum and nuclear industries [5, 6, 7, 8]. This model is derived from conservation laws for each phase for mass, momentum and energy. The phases interact through interfacial terms, some of which are not conservative. These non-conservative terms pose problems for the numerical solution of the model, since numerical schemes for conservation laws take advantage of the conservative nature of the equations. One approach is treating these terms as source terms [4, 9]. The conservative part of the model is then advanced one time step alternatively with the source terms. The latter are solved using ordinary differential equation solvers. The main drawback is that the wave propagation velocities should be affected by the non-conservative terms, which is not properly caught in this approach. The consequence is that the discontinuities that can occur with non-linear models may be smeared. Therefore, many authors have tried to include

*Correspondence to: Department of Energy and Process Engineering, Norwegian University of Science and Technology (NTNU), Kolbjørn Hejes vei 1B, NO-7491 Trondheim, Norway. Email: alexandre.morin [a] sintef.no

them in the framework of the numerical schemes for conservation laws [10, 11, 12, 13]. In the present article, we continue the work presented in [14], making a step in the direction of properly including the non-conservative terms in the numerical scheme for the six-equation two-fluid model by a formulation suitable for the *formally path-consistent* framework of Parés [10]. Castro *et al.* [15] and Abgrall and Karni [16] showed that this approach may produce waves which violate the Rankine-Hugoniot condition. Therefore, in the present work, the propagation of each of the waves has been analysed separately. Though it tends to indicate that the effect shown in [15] and [16] occurs with our scheme, it is marginal. The advantages of being able to treat all terms in a fully upwind manner still make this scheme a better option than solving the non-conservative terms as source terms.

The MUSTA scheme is an option to solve systems of conservation laws [17, 18]. It has been applied to the six-equation two-fluid model [2], and it was shown that it performed well. However, the linearised upwind Roe scheme [19] is generally more accurate. Toumi [3] presented a Roe scheme for the same model, but he made the assumption of incompressible liquid flow. In the present article, we extend the Roe scheme for the six-equation two-fluid model to compressible flows. We show that the Roe averages can be defined independently of the choice of integration path for the non-conservative terms. Therefore we do not concentrate on finding a physically-right path. Further, the derivation of the Roe averages for the variables is mostly analytical and independent of the thermodynamics. Only two remaining scalar relations are dependent on the equation of state. There exist numerical methods to solve those two relations, therefore the scheme can also be used with "black box" thermodynamical routines.

Before we can derive the Roe scheme, we first need to eliminate the non-conservative terms containing time derivatives. This has been achieved by Munkejord *et al.* [2] by transforming the time derivatives into space derivatives. In the present article, we take advantage of this transformation to be able to write the system in quasi-linear form.

In Section 2, we first expose the six-equation two-fluid model. Then in Section 3, we derive the quasilinear expression of the model. In Section 4, the Roe condition is formulated and average formulas that satisfy it are proposed. Next, in Section 5, we explain how we deal with the non-conservative terms. Section 6 points out the resonance which can happen with the present model, and how it is solved. In Section 7, we discuss how to make the scheme second order with the wave limiters. Finally, the numerical scheme is tested on three test cases in Section 8. Section 9 summarises the results of the paper. The main symbols used are listed in Table I. The other ones are introduced in the text.

Table I. Main symbols.

Symbol	Signification
α	Volume fraction
ρ	Density
v	Velocity
e	Internal energy
p	Pressure
Γ	First Grüneisen coefficient
c	Speed of sound
E	Total energy
u_i	Components of the vector $\boldsymbol{U}$
$\boldsymbol{U}$	Vector of the conserved variables
$\boldsymbol{F}$	Vector of the fluxes
$\boldsymbol{W}$	Vector of the non-conservative variables
$\boldsymbol{B}$	Coefficient matrix in the non-conservative terms
$\boldsymbol{S}$	Vector of the algebraic source term
g	Gas phase (Subscript)
ℓ	Liquid phase (Subscript)

DOI: 10.1002/fld

2. THE MODEL

The most common formulation of the six-equation two-fluid model takes the general form [1, 2]

$$\frac{\partial \boldsymbol{U}}{\partial t} + \frac{\partial \boldsymbol{F}(\boldsymbol{U})}{\partial x} + \tilde{\boldsymbol{A}}(\boldsymbol{U})\frac{\partial \tilde{\boldsymbol{V}}(\boldsymbol{U})}{\partial t} + \tilde{\boldsymbol{B}}(\boldsymbol{U})\frac{\partial \tilde{\boldsymbol{W}}(\boldsymbol{U})}{\partial x} = \tilde{\boldsymbol{S}}(\boldsymbol{U}). \tag{1}$$

where the terms $\tilde{\boldsymbol{A}}\partial_t\tilde{\boldsymbol{V}}$ and $\tilde{\boldsymbol{B}}\partial_x\tilde{\boldsymbol{V}}$ are respectively the non-conservative temporal and spatial terms.

The non-conservative temporal term $\tilde{\boldsymbol{A}}\partial_t\tilde{\boldsymbol{V}}$ presents mathematical and numerical difficulties in deriving fully upwind schemes. In this work, we address this difficulty by taking advantage of a mathematically equivalent formulation, derived in [2], that eliminates the non-conservative temporal terms. The system of equations is written as

$$\frac{\partial \boldsymbol{U}}{\partial t} + \frac{\partial \boldsymbol{F}(\boldsymbol{U})}{\partial x} + \boldsymbol{B}'(\boldsymbol{U})\frac{\partial \boldsymbol{W}(\boldsymbol{U})}{\partial x} = \boldsymbol{S}(\boldsymbol{U}), \tag{2}$$

where the variables vector consists of the conserved quantities for each of the two phases (mass, momentum and total energy):

$$\boldsymbol{U} = \begin{bmatrix} u_1 \\ u_2 \\ u_3 \\ u_4 \\ u_5 \\ u_6 \end{bmatrix} = \begin{bmatrix} \alpha_{\mathrm{g}}\rho_{\mathrm{g}} \\ \alpha_\ell\rho_\ell \\ \alpha_{\mathrm{g}}\rho_{\mathrm{g}}v_{\mathrm{g}} \\ \alpha_\ell\rho_\ell v_\ell \\ \alpha_{\mathrm{g}}\rho_{\mathrm{g}}\left(e_{\mathrm{g}} + \frac{1}{2}v_{\mathrm{g}}^2\right) \\ \alpha_\ell\rho_\ell\left(e_\ell + \frac{1}{2}v_\ell^2\right) \end{bmatrix}. \tag{3}$$

Further, the conservative flux $\boldsymbol{F}(\boldsymbol{U})$ was in [2] originally split into a convective part and a pressure part, such that

$$\boldsymbol{F} = \boldsymbol{F}_{\mathrm{c}} + \boldsymbol{F}_{\mathrm{p}} \tag{4}$$

with

$$\boldsymbol{F}_{\mathrm{c}}(\boldsymbol{U}) = \begin{bmatrix} \alpha_{\mathrm{g}}\rho_{\mathrm{g}}v_{\mathrm{g}} \\ \alpha_\ell\rho_\ell v_\ell \\ \alpha_{\mathrm{g}}\rho_{\mathrm{g}}v_{\mathrm{g}}^2 \\ \alpha_\ell\rho_\ell v_\ell^2 \\ \alpha_{\mathrm{g}}\rho_{\mathrm{g}}v_{\mathrm{g}}\left(e_{\mathrm{g}} + \frac{1}{2}v_{\mathrm{g}}^2\right) \\ \alpha_\ell\rho_\ell v_\ell\left(e_\ell + \frac{1}{2}v_\ell^2\right) \end{bmatrix} \quad \text{and} \quad \boldsymbol{F}_p(\boldsymbol{U}) = \begin{bmatrix} 0 \\ 0 \\ 0 \\ 0 \\ \alpha_{\mathrm{g}}v_{\mathrm{g}}p \\ \alpha_\ell v_\ell p \end{bmatrix}. \tag{5}$$

However, in the present work, we obtain a simpler non-conservative system by modifying $\boldsymbol{B}'(\boldsymbol{U})$ to also incorporate the pressure part of the flux $\boldsymbol{F}_p(\boldsymbol{U})$. By this, we obtain the equivalent formulation of the system presented in [2]:

$$\frac{\partial \boldsymbol{U}}{\partial t} + \frac{\partial \boldsymbol{F}_c(\boldsymbol{U})}{\partial x} + \boldsymbol{B}(\boldsymbol{U})\frac{\partial \boldsymbol{W}(\boldsymbol{U})}{\partial x} = \boldsymbol{S}(\boldsymbol{U}), \tag{6}$$

where

$$\boldsymbol{B}(\boldsymbol{U}) = \begin{bmatrix} 0 & 0 & 0 \\ 0 & 0 & 0 \\ \alpha_{\mathrm{g}} & 0 & \Delta p \\ \alpha_\ell & 0 & -\Delta p \\ \alpha_{\mathrm{g}}v_{\mathrm{g}} - \eta\alpha_{\mathrm{g}}\alpha_\ell\left(v_{\mathrm{g}} - v_\ell\right) & \eta\rho_\ell\alpha_{\mathrm{g}}c_\ell^2 & v_\tau\Delta p \\ \alpha_\ell v_\ell + \eta\alpha_{\mathrm{g}}\alpha_\ell\left(v_{\mathrm{g}} - v_\ell\right) & \eta\rho_{\mathrm{g}}\alpha_\ell c_{\mathrm{g}}^2 & -v_\tau\Delta p \end{bmatrix} \tag{7}$$

and

$$\boldsymbol{W}(\boldsymbol{U}) = \begin{bmatrix} p \\ \alpha_{\mathrm{g}}v_{\mathrm{g}} + \alpha_\ell v_\ell \\ \alpha_{\mathrm{g}} \end{bmatrix}. \tag{8}$$

DOI: 10.1002/fld

where η is defined by

$$\eta = \frac{p}{\rho_\mathrm{g}\alpha_\ell c_\mathrm{g}^2 + \rho_\ell \alpha_\mathrm{g} c_\ell^2}. \tag{9}$$

It is well known that the basic equal-pressure two-fluid model is not hyperbolic [1, 20]. Therefore, our present model includes the regularisation terms Δp and v_τ that make it hyperbolic, often used for numerical testing [3, 4, 6, 9, 21, 22]. They can for example represent surface tension or hydrostatics. In this work, we focused on the numerical scheme, and therefore did not emphasise the physical relevance of the model closure relations. The discussions in the present article remain nevertheless relevant for any other choice of interfacial pressure regularisation term. We chose a widely used term [2, 4, 22, 23, 24] derived from mathematical considerations [25, 26]

$$\Delta p = \delta \frac{\alpha_\mathrm{g}\alpha_\ell\rho_\mathrm{g}\rho_\ell(v_\mathrm{g} - v_\ell)^2}{\alpha_\ell\rho_\mathrm{g} + \alpha_\mathrm{g}\rho_\ell}. \tag{10}$$

When the parameter δ is equal to one, this is the minimum pressure difference between the phases necessary to make the model hyperbolic at the first order of $(v_\mathrm{g} - v_\ell)$. It has been shown for some particular cases of the two-fluid six-equation model [25, 26], and for the two-fluid four-equation model without energy equations [22]. It can be shown with a perturbation method that it is also true for the general two-fluid six-equation model. With δ larger than one, the model is hyperbolic in an interval $|v_\mathrm{g} - v_\ell| < \Omega$, where Ω is some constant dependent on δ. The other term is defined by

$$v_\tau = \frac{\alpha_\ell\Gamma_\mathrm{g}v_\mathrm{g} + \alpha_\mathrm{g}\Gamma_\ell v_\ell}{\alpha_\ell\Gamma_\mathrm{g} + \alpha_\mathrm{g}\Gamma_\ell}. \tag{11}$$

Finally, the source term $\boldsymbol{S}(\boldsymbol{U})$ can represent gravity or phase interactions.

3. QUASILINEAR FORM

In order to derive a Roe scheme [19], we first write the model in a quasilinear form:

$$\frac{\partial \boldsymbol{U}}{\partial t} + \boldsymbol{A}(\boldsymbol{U})\frac{\partial \boldsymbol{U}}{\partial x} = \boldsymbol{S}(\boldsymbol{U}), \tag{12}$$

where

$$\boldsymbol{A}(\boldsymbol{U}) = \frac{\partial \boldsymbol{F}_c}{\partial \boldsymbol{U}} + \boldsymbol{B}(\boldsymbol{U})\frac{\partial \boldsymbol{W}}{\partial \boldsymbol{U}}. \tag{13}$$

To achieve this, we first derive the analytical Jacobian matrix of the flux. A natural decomposition of the problem is to treat the convective part $\boldsymbol{F}_c$ separately from the rest of the flux, mainly involving the pressure, $\boldsymbol{B}(\boldsymbol{U})\frac{\partial \boldsymbol{W}(\boldsymbol{U})}{\partial x}$. The resulting Jacobian matrices will be called $\boldsymbol{A}_c$ and $\boldsymbol{A}_p$, respectively.

3.1. Convective part

We can write the following differentials

$$\alpha_\mathrm{g}\rho_\mathrm{g}\,\mathrm{d}v_\mathrm{g} = \mathrm{d}u_3 - v_\mathrm{g}\,\mathrm{d}u_1 \tag{14}$$

$$\alpha_\ell\rho_\ell\,\mathrm{d}v_\ell = \mathrm{d}u_4 - v_\ell\,\mathrm{d}u_2 \tag{15}$$

and the matrix $\boldsymbol{A}_c$ follows

$$\boldsymbol{A}_c = \frac{\partial \boldsymbol{F}_c}{\partial \boldsymbol{U}} = \begin{bmatrix} 0 & 0 & 1 & 0 & 0 & 0 \\ 0 & 0 & 0 & 1 & 0 & 0 \\ -v_\mathrm{g}^2 & 0 & 2v_\mathrm{g} & 0 & 0 & 0 \\ 0 & -v_\ell^2 & 0 & 2v_\ell & 0 & 0 \\ -v_\mathrm{g}E_\mathrm{g} & 0 & E_\mathrm{g} & 0 & v_\mathrm{g} & 0 \\ 0 & -v_\ell E_\ell & 0 & E_\ell & 0 & v_\ell \end{bmatrix} \tag{16}$$

DOI: 10.1002/fld

where $E_\varphi = e_\varphi + \frac{1}{2}v_\varphi^2$.

3.2. A pressure differential

In order to derive the Jacobian $\boldsymbol{A}_p$ of the pressure flux, we need the derivative of the non-conservative flux variables, $\boldsymbol{W}$, with respect to the conservative variables, $\boldsymbol{U}$. First, some useful differentials are derived. We know from [2] that the differential of the pressure can be written

$$\mathrm{d}p = \left(c_k^2 - \Gamma_k \frac{p}{\rho_k}\right)\mathrm{d}\rho_k + \Gamma_k \rho_k \,\mathrm{d}e_k, \tag{17}$$

or equivalently:

$$\mathrm{d}p = \left(c_k^2 - \Gamma_k \left(e_k + \frac{p}{\rho_k}\right)\right)\mathrm{d}\rho_k + \Gamma_k \,\mathrm{d}(\rho_k e_k) \tag{18}$$

for $\mathrm{k} \in \mathrm{g}, \ell$. Furthermore,

$$\mathrm{d}\alpha_k = \frac{1}{\rho_k}\left(\mathrm{d}(\alpha_k\rho_k) - \alpha_k \,\mathrm{d}\rho_k\right) \tag{19}$$

$$= \frac{1}{\rho_k e_k}\left(\mathrm{d}(\alpha_k\rho_k e_k) - \alpha_k \,\mathrm{d}(\rho_k e_k)\right), \tag{20}$$

and similarly

$$\mathrm{d}\rho_k = \frac{1}{\alpha_k}\left(\mathrm{d}(\alpha_k\rho_k) - \rho_k \,\mathrm{d}\alpha_k\right), \tag{21}$$

$$\mathrm{d}(\rho_k e_k) = \frac{1}{\alpha_k}\left(\mathrm{d}(\alpha_k\rho_k e_k) - \rho_k e_k \,\mathrm{d}\alpha_k\right). \tag{22}$$

Hence we can write the differential (18) as

$$\alpha_k \,\mathrm{d}p = \left(c_k^2 - \Gamma_k \left(e_k + \frac{p}{\rho_k}\right)\right)\left(\mathrm{d}(\alpha_k\rho_k) - \rho_k \,\mathrm{d}\alpha_k\right) + \Gamma_k \left(\mathrm{d}(\alpha_k\rho_k e_k) - \rho_k e_k \,\mathrm{d}\alpha_k\right) \tag{23}$$

which simplifies to

$$\alpha_k \,\mathrm{d}p = \left(c_k^2 - \Gamma_k \left(e_k + \frac{p}{\rho_k}\right)\right)\mathrm{d}(\alpha_k\rho_k) + \Gamma_k \,\mathrm{d}(\alpha_k\rho_k e_k) - \zeta_k \,\mathrm{d}\alpha_k. \tag{24}$$

Now we express (24) for $\mathrm{k} = \mathrm{g}$ and $\mathrm{k} = \ell$, multiply them respectively by ζ_ℓ and ζ_g and add them to eliminate $\mathrm{d}\alpha_\mathrm{g}$

$$\mathcal{R}\,\mathrm{d}p = \zeta_\ell\left(\frac{\zeta_\mathrm{g}}{\rho_\mathrm{g}} - \Gamma_\mathrm{g} e_\mathrm{g}\right)\mathrm{d}u_1 + \zeta_\ell\Gamma_\mathrm{g}\,\mathrm{d}(u_1 e_\mathrm{g}) + \zeta_\mathrm{g}\left(\frac{\zeta_\ell}{\rho_\ell} - \Gamma_\ell e_\ell\right)\mathrm{d}u_2 + \zeta_\mathrm{g}\Gamma_\ell\,\mathrm{d}(u_2 e_\ell), \tag{25}$$

and in terms of the elements of the state vector $\boldsymbol{U}$, the pressure differential is

$$\mathcal{R}\,\mathrm{d}p = \zeta_\ell\beta_\mathrm{g}\,\mathrm{d}u_1 + \zeta_\mathrm{g}\beta_\ell\,\mathrm{d}u_2 - \zeta_\ell\Gamma_\mathrm{g}v_\mathrm{g}\,\mathrm{d}u_3 - \zeta_\mathrm{g}\Gamma_\ell v_\ell\,\mathrm{d}u_4 + \zeta_\ell\Gamma_\mathrm{g}\,\mathrm{d}u_5 + \zeta_\mathrm{g}\Gamma_\ell\,\mathrm{d}u_6, \tag{26}$$

where

$$\zeta_k = \rho_k c_k^2 - \Gamma_k p, \tag{27}$$

$$\beta_k = c_k^2 - \Gamma_k\left(e_k + \frac{p}{\rho_k}\right) + \frac{1}{2}\Gamma_k v_k^2, \tag{28}$$

$$\mathcal{R} = \alpha_\mathrm{g}\zeta_\ell + \alpha_\ell\zeta_\mathrm{g}. \tag{29}$$

DOI: 10.1002/fld

3.3. A volume-fraction differential

Now, we derive a volume-fraction differential. We start from

$$\mathrm{d}u_1 = \rho_\mathrm{g}\,\mathrm{d}\alpha_\mathrm{g} + \alpha_\mathrm{g}\,\mathrm{d}\rho_\mathrm{g}, \tag{30}$$

in which we substitute the density differential extracted from (17)

$$\mathrm{d}u_1 = \rho_\mathrm{g}\,\mathrm{d}\alpha_\mathrm{g} + \frac{\alpha_\mathrm{g}\rho_\mathrm{g}}{\rho_\mathrm{g}c_\mathrm{g}^2 - p\Gamma_\mathrm{g}}\left(\mathrm{d}p - \Gamma_\mathrm{g}\rho_\mathrm{g}\,\mathrm{d}e_\mathrm{g}\right). \tag{31}$$

Now, through the expression of the pressure differential (25) and $\mathrm{d}(u_1e_\mathrm{g}) = u_1\,\mathrm{d}e_\mathrm{g} + e_\mathrm{g}\,\mathrm{d}u_1$, we obtain

$$\mathcal{R}\,\mathrm{d}\alpha_\mathrm{g} = \alpha_\ell\left(\frac{\zeta_\mathrm{g}}{\rho_\mathrm{g}} - \Gamma_\mathrm{g}e_\mathrm{g}\right)\mathrm{d}u_1 - \alpha_\mathrm{g}\left(\frac{\zeta_\ell}{\rho_\ell} - \Gamma_\ell e_\ell\right)\mathrm{d}u_2 + \alpha_\ell\Gamma_\mathrm{g}\,\mathrm{d}(u_1e_\mathrm{g}) - \alpha_\mathrm{g}\Gamma_\ell\,\mathrm{d}(u_2e_\ell), \tag{32}$$

and in terms of the elements of the state vector $\boldsymbol{U}$, the volume-fraction differential is

$$\mathcal{R}\,\mathrm{d}\alpha_\mathrm{g} = \alpha_\ell\beta_\mathrm{g}\,\mathrm{d}u_1 - \alpha_\mathrm{g}\beta_\ell\,\mathrm{d}u_2 - \alpha_\ell\Gamma_\mathrm{g}v_\mathrm{g}\,\mathrm{d}u_3 - \alpha_\mathrm{g}\Gamma_\ell v_\ell\,\mathrm{d}u_4 + \alpha_\ell\Gamma_\mathrm{g}\,\mathrm{d}u_5 - \alpha_\mathrm{g}\Gamma_\ell\,\mathrm{d}u_6. \tag{33}$$

3.4. Velocity differentials

Finally, through the volume-fraction differential (33) and

$$\mathrm{d}v_\mathrm{g} = \frac{1}{\alpha_\mathrm{g}\rho_\mathrm{g}}\left(\mathrm{d}u_3 - v_\mathrm{g}\,\mathrm{d}u_1\right), \tag{34}$$

$$\mathrm{d}v_\ell = \frac{1}{\alpha_\ell\rho_\ell}\left(\mathrm{d}u_4 - v_\ell\,\mathrm{d}u_2\right), \tag{35}$$

we obtain the following differentials

$$\begin{aligned}\mathcal{R}\,\mathrm{d}(\alpha_\mathrm{g}v_\mathrm{g}) = {} & v_\mathrm{g}\left(\alpha_\ell\beta_\mathrm{g} - \frac{\mathcal{R}}{\rho_\mathrm{g}}\right)\mathrm{d}u_1 - \alpha_\mathrm{g}\beta_\ell v_\mathrm{g}\,\mathrm{d}u_2 \\ & + \left(\frac{\mathcal{R}}{\rho_\mathrm{g}} - \alpha_\ell\Gamma_\mathrm{g}v_\mathrm{g}^2\right)\mathrm{d}u_3 + \alpha_\mathrm{g}\Gamma_\ell v_\mathrm{g}v_\ell\,\mathrm{d}u_4 + \alpha_\ell\Gamma_\mathrm{g}v_\mathrm{g}\,\mathrm{d}u_5 - \alpha_\mathrm{g}\Gamma_\ell v_\mathrm{g}\,\mathrm{d}u_6,\end{aligned} \tag{36}$$

$$\begin{aligned}\mathcal{R}\,\mathrm{d}(\alpha_\ell v_\ell) = {} & -\alpha_\ell\beta_\mathrm{g}v_\ell\,\mathrm{d}u_1 + v_\ell\left(\alpha_\mathrm{g}\beta_\ell - \frac{\mathcal{R}}{\rho_\ell}\right)\mathrm{d}u_2 \\ & + \alpha_\ell\Gamma_\mathrm{g}v_\mathrm{g}v_\ell\,\mathrm{d}u_3 + \left(\frac{\mathcal{R}}{\rho_\ell} - \alpha_\mathrm{g}\Gamma_\ell v_\ell^2\right)\mathrm{d}u_4 - \alpha_\ell\Gamma_\mathrm{g}v_\ell\,\mathrm{d}u_5 + \alpha_\mathrm{g}\Gamma_\ell v_\ell\,\mathrm{d}u_6.\end{aligned} \tag{37}$$

3.5. Pressure part

With the help of the differentials (26), (33), (36) and (37), we can write the Jacobian matrix of $\boldsymbol{W}$ defined in (7)

$$\boldsymbol{M} = \frac{\partial \boldsymbol{W}\left(\boldsymbol{U}\right)}{\partial \boldsymbol{U}} = \mathcal{R}^{-1}\begin{bmatrix} \zeta_\ell\beta_\mathrm{g} & \left(v_\mathrm{g} - v_\ell\right)\alpha_\ell\beta_\mathrm{g} - \mathcal{R}v_\mathrm{g}/\rho_\mathrm{g} & \alpha_\ell\beta_\mathrm{g} \\ \zeta_\mathrm{g}\beta_\ell & \left(v_\ell - v_\mathrm{g}\right)\alpha_\mathrm{g}\beta_\ell - \mathcal{R}v_\ell/\rho_\ell & -\alpha_\mathrm{g}\beta_\ell \\ -\zeta_\ell\Gamma_\mathrm{g}v_\mathrm{g} & \mathcal{R}/\rho_\mathrm{g} - \left(v_\mathrm{g} - v_\ell\right)\alpha_\ell\Gamma_\mathrm{g}v_\mathrm{g} & -\alpha_\ell\Gamma_\mathrm{g}v_\mathrm{g} \\ -\zeta_\mathrm{g}\Gamma_\ell v_\ell & \mathcal{R}/\rho_\ell - \left(v_\ell - v_\mathrm{g}\right)\alpha_\mathrm{g}\Gamma_\ell v_\ell & \alpha_\mathrm{g}\Gamma_\ell v_\ell \\ \zeta_\ell\Gamma_\mathrm{g} & \left(v_\mathrm{g} - v_\ell\right)\alpha_\ell\Gamma_\mathrm{g} & \alpha_\ell\Gamma_\mathrm{g} \\ \zeta_\mathrm{g}\Gamma_\ell & \left(v_\ell - v_\mathrm{g}\right)\alpha_\mathrm{g}\Gamma_\ell & -\alpha_\mathrm{g}\Gamma_\ell \end{bmatrix}^T, \tag{38}$$

The matrix $\boldsymbol{A}_p$ is defined as

$$\boldsymbol{A}_p = \mathcal{R}\boldsymbol{B}(\boldsymbol{U})\frac{\partial \boldsymbol{W}(\boldsymbol{U})}{\partial \boldsymbol{U}} = \mathcal{R}\boldsymbol{B}\boldsymbol{M}, \tag{39}$$

such that the Jacobian matrix $\boldsymbol{A}$ is

$$\boldsymbol{A} = \boldsymbol{A}_c + \mathcal{R}^{-1}\boldsymbol{A}_p. \tag{40}$$

DOI: 10.1002/fld

4. THE ROE SCHEME

The Roe scheme requires the construction of a matrix at each cell interface. One seeks here the Jacobian matrix $\boldsymbol{A}$ evaluated at a particular average of the variables in the neighbouring cells. This is called Roe averaging and denoted by $\hat{\boldsymbol{A}}$ in the following. It has to satisfy some conditions [19, 22, 27, 28],

- R1: $\hat{\boldsymbol{A}}\left(\boldsymbol{U}^{\mathrm{L}},\boldsymbol{U}^{\mathrm{R}}\right)$ is diagonalisable with real eigenvalues,
- R2: $\hat{\boldsymbol{A}}\left(\boldsymbol{U}^{\mathrm{L}},\boldsymbol{U}^{\mathrm{R}}\right)\rightarrow\boldsymbol{A}\left(\bar{\boldsymbol{U}}\right)$ smoothly as $\boldsymbol{U}^{\mathrm{L}},\boldsymbol{U}^{\mathrm{R}}\rightarrow\bar{\boldsymbol{U}}$,
- R3: $\hat{\boldsymbol{A}}\left(\boldsymbol{U}^{\mathrm{L}},\boldsymbol{U}^{\mathrm{R}}\right)\left(\boldsymbol{U}^{\mathrm{R}}-\boldsymbol{U}^{\mathrm{L}}\right)=$

$$\boldsymbol{F}_c(\boldsymbol{U}^{\mathrm{R}})-\boldsymbol{F}_c(\boldsymbol{U}^{\mathrm{L}})+\overline{\boldsymbol{B}}\left(\boldsymbol{U}^{\mathrm{L}},\boldsymbol{U}^{\mathrm{R}}\right)\left(\boldsymbol{W}(\boldsymbol{U}^{\mathrm{R}})-\boldsymbol{W}(\boldsymbol{U}^{\mathrm{L}})\right).$$

The condition R3 is found by using the definition of $\overline{\boldsymbol{B}}$ in [2] in the Roe condition in [27]. The condition R1 will be fulfilled as long as the matrix $\hat{\boldsymbol{A}}(\boldsymbol{U}^{\mathrm{L}},\boldsymbol{U}^{\mathrm{R}})$ is defined as the matrix $\boldsymbol{A}(\hat{\boldsymbol{U}})$ evaluated for some Roe-average state $\hat{\boldsymbol{U}}$ of the left and right states $\boldsymbol{U}^{\mathrm{L}}$ and $\boldsymbol{U}^{\mathrm{R}}$, and that $\hat{\boldsymbol{U}}$ is within the hyperbolic domain of the model. R2 will in this case also be trivially fulfilled. However, the condition R3 is problematic. Note that the matrix $\overline{\boldsymbol{B}}$ is a property of the path chosen to evaluate the non-conservative products, and is independent of the numerical method [2]. Specifically, it will be shown in Section 4.2 that $\overline{\boldsymbol{B}}$ disappears from condition R3, so that the Roe averages can be defined independently of $\overline{\boldsymbol{B}}$. In this section, it is assumed that it is known. It will be discussed in Section 5.

Similarly to what was done in the derivation of the Jacobian matrix, we can split the problem into a convective part and a pressure part, such that $\hat{\boldsymbol{A}}=\hat{\boldsymbol{A}}_c+\hat{\mathcal{R}}^{-1}\hat{\boldsymbol{A}}_p$. Then we can remark that if the subconditions

$$\hat{\boldsymbol{A}}_c\left(\boldsymbol{U}^{\mathrm{L}},\boldsymbol{U}^{\mathrm{R}}\right)\left(\boldsymbol{U}^{\mathrm{R}}-\boldsymbol{U}^{\mathrm{L}}\right)=\boldsymbol{F}_c(\boldsymbol{U}^{\mathrm{R}})-\boldsymbol{F}_c(\boldsymbol{U}^{\mathrm{L}}), \tag{41}$$

$$\hat{\mathcal{R}}^{-1}\hat{\boldsymbol{A}}_p\left(\boldsymbol{U}^{\mathrm{L}},\boldsymbol{U}^{\mathrm{R}}\right)\left(\boldsymbol{U}^{\mathrm{R}}-\boldsymbol{U}^{\mathrm{L}}\right)=\overline{\boldsymbol{B}}\left(\boldsymbol{U}^{\mathrm{L}},\boldsymbol{U}^{\mathrm{R}}\right)\left(\boldsymbol{W}(\boldsymbol{U}^{\mathrm{R}})-\boldsymbol{W}(\boldsymbol{U}^{\mathrm{L}})\right) \tag{42}$$

are fulfilled, then the Roe condition R3 will be fulfilled. Therefore, we choose to split R3 in two, (41) and (42), and to build the partial matrices $\hat{\boldsymbol{A}}_c$ and $\hat{\boldsymbol{A}}_p$ that satisfy each its own condition, so that $\hat{\boldsymbol{A}}$ will satisfy R3.

4.1. Convective part

The derivation of the Roe matrix for the convective part $\hat{\boldsymbol{A}}_c$ is already well known, using the parameter-vector approach of Roe [19]. Specifically, Toumi [3] gives the parameter vector for this case. The condition (41) is fulfilled for a matrix $\hat{\boldsymbol{A}}_c$ defined as the matrix $\boldsymbol{A}_c$ (16) evaluated for the following Roe-averages of the velocity and the internal energy

$$\hat{v}_k=\frac{\left(\sqrt{\alpha_k\rho_k}v_k\right)^{\mathrm{L}}+\left(\sqrt{\alpha_k\rho_k}v_k\right)^{\mathrm{R}}}{\left(\sqrt{\alpha_k\rho_k}\right)^{\mathrm{L}}+\left(\sqrt{\alpha_k\rho_k}\right)^{\mathrm{R}}}, \tag{43}$$

$$\hat{e}_k=\tilde{e}_k+\frac{1}{2}\frac{\sqrt{(\alpha_k\rho_k)^{\mathrm{L}}(\alpha_k\rho_k)^{\mathrm{R}}}\left(v_k^{\mathrm{R}}-v_k^{\mathrm{L}}\right)^2}{\left(\left(\sqrt{\alpha_k\rho_k}\right)^{\mathrm{L}}+\left(\sqrt{\alpha_k\rho_k}\right)^{\mathrm{R}}\right)^2} \tag{44}$$

where

$$\tilde{e}_k=\frac{\left(\sqrt{\alpha_k\rho_k}e_k\right)^{\mathrm{L}}+\left(\sqrt{\alpha_k\rho_k}e_k\right)^{\mathrm{R}}}{\left(\sqrt{\alpha_k\rho_k}\right)^{\mathrm{L}}+\left(\sqrt{\alpha_k\rho_k}\right)^{\mathrm{R}}}. \tag{45}$$

DOI: 10.1002/fld

4.2. Relation for the pressure part

On the other hand, the parameter-vector approach is impractical for the pressure part. Instead, we follow a strategy similar to that in [29]. It consists in reducing the partial Roe condition (42) on $\hat{\boldsymbol{A}}_p$ to two scalar ones. One will concern the pressure average, and the other the mixture-velocity average. This approach will give analytical averaging formulas for all the variables but the pressure, for which we will have a relation to satisfy. This relation will be dependent on the equation of state and will generally have to be solved numerically. Thus we can construct a partially analytical Roe matrix for any equation of state.

By analogy with the the definition of $\boldsymbol{A}_p$ in (39), we look for $\hat{\boldsymbol{A}}_p$ in the form $\hat{\boldsymbol{A}}_p = \hat{\mathcal{R}}\overline{\boldsymbol{B}}\hat{\boldsymbol{M}}$. Inserting this into (42) gives

$$\hat{\boldsymbol{M}}\left(\boldsymbol{U}^{\mathrm{L}}, \boldsymbol{U}^{\mathrm{R}}\right)\left(\boldsymbol{U}^{\mathrm{R}} - \boldsymbol{U}^{\mathrm{L}}\right) = \boldsymbol{W}(\boldsymbol{U}^{\mathrm{R}}) - \boldsymbol{W}(\boldsymbol{U}^{\mathrm{L}}), \tag{46}$$

which results in a system of three equations. The matrix $\overline{\boldsymbol{B}}$ disappears from this system, therefore the Roe condition R3 can be satisfied without making any assumption on how $\boldsymbol{B}$ is averaged. Thus the Roe scheme can be derived independently of the choice of the non-conservative term averaging.

4.3. Velocity average for the pressure part

The first line of the system (46) reads

$$\begin{aligned}\hat{\mathcal{R}}\left(p^{\mathrm{R}} - p^{\mathrm{L}}\right) = {}& \hat{\zeta}_\ell\hat{\beta}_{\mathrm{g}}\left(u_1^{\mathrm{R}} - u_1^{\mathrm{L}}\right) + \hat{\zeta}_{\mathrm{g}}\hat{\beta}_\ell\left(u_2^{\mathrm{R}} - u_2^{\mathrm{L}}\right) - \hat{\zeta}_\ell\hat{\Gamma}_{\mathrm{g}}\hat{v}_{\mathrm{g}}\left(u_3^{\mathrm{R}} - u_3^{\mathrm{L}}\right) \\ & - \hat{\zeta}_{\mathrm{g}}\hat{\Gamma}_\ell\hat{v}_\ell\left(u_4^{\mathrm{R}} - u_4^{\mathrm{L}}\right) + \hat{\zeta}_\ell\hat{\Gamma}_{\mathrm{g}}\left(u_5^{\mathrm{R}} - u_5^{\mathrm{L}}\right) + \hat{\zeta}_{\mathrm{g}}\hat{\Gamma}_\ell\left(u_6^{\mathrm{R}} - u_6^{\mathrm{L}}\right).\end{aligned} \tag{47}$$

When the velocities are averaged following the formula (43), and if we choose

$$\hat{\beta}_k = \frac{\hat{\zeta}_k}{\hat{\rho}_k} - \hat{\Gamma}_k\left(\tilde{e}_k - \frac{1}{2}\hat{v}_k^2\right), \tag{48}$$

this expression is equivalent to the "Roe-average" of the pressure differential (25)

$$\begin{aligned}&\hat{\mathcal{R}}\left(p^{\mathrm{R}} - p^{\mathrm{L}}\right) = \\ &\quad\hat{\zeta}_\ell\left(\widehat{\left(\frac{\zeta_{\mathrm{g}}}{\rho_{\mathrm{g}}}\right)} - \hat{\Gamma}_{\mathrm{g}}\tilde{e}_{\mathrm{g}}\right)\left((\alpha_{\mathrm{g}}\rho_{\mathrm{g}})^{\mathrm{R}} - (\alpha_{\mathrm{g}}\rho_{\mathrm{g}})^{\mathrm{L}}\right) + \hat{\zeta}_{\mathrm{g}}\left(\widehat{\left(\frac{\zeta_\ell}{\rho_\ell}\right)} - \hat{\Gamma}_\ell\tilde{e}_\ell\right)\left((\alpha_\ell\rho_\ell)^{\mathrm{R}} - (\alpha_\ell\rho_\ell)^{\mathrm{L}}\right) \\ &\qquad + \hat{\zeta}_\ell\hat{\Gamma}_{\mathrm{g}}\left((\alpha_{\mathrm{g}}\rho_{\mathrm{g}}e_{\mathrm{g}})^{\mathrm{R}} - (\alpha_{\mathrm{g}}\rho_{\mathrm{g}}e_{\mathrm{g}})^{\mathrm{L}}\right) + \hat{\zeta}_{\mathrm{g}}\hat{\Gamma}_\ell\left((\alpha_\ell\rho_\ell e_\ell)^{\mathrm{R}} - (\alpha_\ell\rho_\ell e_\ell)^{\mathrm{L}}\right)\end{aligned} \tag{49}$$

Proof
Equating the right-hand sides of (47) and (49), as well as using (48) and

$$u_5 = u_1 e_{\mathrm{g}} + \frac{1}{2}u_1 v_{\mathrm{g}}^2, \tag{50}$$

$$u_6 = u_2 e_\ell + \frac{1}{2}u_2 v_\ell^2, \tag{51}$$

we obtain

$$\begin{aligned}&\frac{1}{2}\hat{\zeta}_\ell\hat{\Gamma}_{\mathrm{g}}\hat{v}_{\mathrm{g}}^2\left((\alpha_{\mathrm{g}}\rho_{\mathrm{g}})^{\mathrm{R}} - (\alpha_{\mathrm{g}}\rho_{\mathrm{g}})^{\mathrm{L}}\right) + \frac{1}{2}\hat{\zeta}_{\mathrm{g}}\hat{\Gamma}_\ell\hat{v}_\ell^2\left((\alpha_\ell\rho_\ell)^{\mathrm{R}} - (\alpha_\ell\rho_\ell)^{\mathrm{L}}\right) \\ &\qquad - \hat{\zeta}_\ell\hat{\Gamma}_{\mathrm{g}}\hat{v}_{\mathrm{g}}\left((\alpha_{\mathrm{g}}\rho_{\mathrm{g}}v_{\mathrm{g}})^{\mathrm{R}} - (\alpha_{\mathrm{g}}\rho_{\mathrm{g}}v_{\mathrm{g}})^{\mathrm{L}}\right) - \hat{\zeta}_{\mathrm{g}}\hat{\Gamma}_\ell\hat{v}_\ell\left((\alpha_\ell\rho_\ell v_\ell)^{\mathrm{R}} - (\alpha_\ell\rho_\ell v_\ell)^{\mathrm{L}}\right) \\ &\qquad + \frac{1}{2}\hat{\zeta}_\ell\hat{\Gamma}_{\mathrm{g}}\left((\alpha_{\mathrm{g}}\rho_{\mathrm{g}}v_{\mathrm{g}}^2)^{\mathrm{R}} - (\alpha_{\mathrm{g}}\rho_{\mathrm{g}}v_{\mathrm{g}}^2)^{\mathrm{L}}\right) + \frac{1}{2}\hat{\zeta}_{\mathrm{g}}\hat{\Gamma}_\ell\left((\alpha_\ell\rho_\ell v_\ell^2)^{\mathrm{R}} - (\alpha_\ell\rho_\ell v_\ell^2)^{\mathrm{L}}\right) = 0.\end{aligned} \tag{52}$$

DOI: 10.1002/fld

which is satisfied if

$$\frac{1}{2}\hat{\zeta}_\ell\hat{\Gamma}_{\rm g}\hat{v}_{\rm g}^2\left((\alpha_{\rm g}\rho_{\rm g})^{\rm R}-(\alpha_{\rm g}\rho_{\rm g})^{\rm L}\right)-\hat{\zeta}_\ell\hat{\Gamma}_{\rm g}\hat{v}_{\rm g}\left((\alpha_{\rm g}\rho_{\rm g}v_{\rm g})^{\rm R}-(\alpha_{\rm g}\rho_{\rm g}v_{\rm g})^{\rm L}\right)$$
$$+\frac{1}{2}\hat{\zeta}_\ell\hat{\Gamma}_{\rm g}\left((\alpha_{\rm g}\rho_{\rm g}v_{\rm g}^2)^{\rm R}-(\alpha_{\rm g}\rho_{\rm g}v_{\rm g}^2)^{\rm L}\right)=0 \quad (53)$$

and

$$\frac{1}{2}\hat{\zeta}_{\rm g}\hat{\Gamma}_\ell\hat{v}_\ell^2\left((\alpha_\ell\rho_\ell)^{\rm R}-(\alpha_\ell\rho_\ell)^{\rm L}\right)-\hat{\zeta}_{\rm g}\hat{\Gamma}_\ell\hat{v}_\ell\left((\alpha_\ell\rho_\ell v_\ell)^{\rm R}-(\alpha_\ell\rho_\ell v_\ell)^{\rm L}\right)$$
$$+\frac{1}{2}\hat{\zeta}_{\rm g}\hat{\Gamma}_\ell\left((\alpha_\ell\rho_\ell v_\ell^2)^{\rm R}-(\alpha_\ell\rho_\ell v_\ell^2)^{\rm L}\right)=0 \quad (54)$$

hold independently. They simplify to

$$\hat{v}_{\rm g}^2\left((\alpha_{\rm g}\rho_{\rm g})^{\rm R}-(\alpha_{\rm g}\rho_{\rm g})^{\rm L}\right)-2\left((\alpha_{\rm g}\rho_{\rm g}v_{\rm g})^{\rm R}-(\alpha_{\rm g}\rho_{\rm g}v_{\rm g})^{\rm L}\right)+\left((\alpha_{\rm g}\rho_{\rm g}v_{\rm g}^2)^{\rm R}-(\alpha_{\rm g}\rho_{\rm g}v_{\rm g}^2)^{\rm L}\right)=0 \quad (55)$$

and

$$\hat{v}_\ell^2\left((\alpha_\ell\rho_\ell)^{\rm R}-(\alpha_\ell\rho_\ell)^{\rm L}\right)-2\left((\alpha_\ell\rho_\ell v_\ell)^{\rm R}-(\alpha_\ell\rho_\ell v_\ell)^{\rm L}\right)+\left((\alpha_\ell\rho_\ell v_\ell^2)^{\rm R}-(\alpha_\ell\rho_\ell v_\ell^2)^{\rm L}\right)=0 \quad (56)$$

which in turn are satisfied if the velocity follows the averaging formula (43). □

4.4. Further simplification of the first line of the system (46)

Let us assume that the averages are such that the following equalities hold

$$(\alpha_k\rho_k)^{\rm R}-(\alpha_k\rho_k)^{\rm L}=\hat{\alpha_k}\left(\rho_k^{\rm R}-\rho_k^{\rm L}\right)+\hat{\rho_k}\left(\alpha_k^{\rm R}-\alpha_k^{\rm L}\right), \quad (57)$$
$$(\alpha_k\rho_k e_k)^{\rm R}-(\alpha_k\rho_k e_k)^{\rm L}=\hat{\alpha}_k\left((\rho_k e_k)^{\rm R}-(\rho_k e_k)^{\rm L}\right)+\hat{\rho}_k\tilde{e}_k\left(\alpha_k^{\rm R}-\alpha_k^{\rm L}\right). \quad (58)$$
$$(59)$$

We also observe that

$$(\rho_k e_k)^{\rm R}-(\rho_k e_k)^{\rm L}=\breve{\rho}_k\left(e_k^{\rm R}-e_k^{\rm L}\right)+\tilde{e}_k\left(\rho_k^{\rm R}-\rho_k^{\rm L}\right), \quad (60)$$

where $\tilde{e}_k$ is given by (45) and

$$\breve{\rho}_k=\frac{\rho_k^{\rm L}\rho_k^{\rm R}}{\hat{\rho}_k}. \quad (61)$$

Now, through the definition

$$\widehat{\left(\frac{\zeta_k}{\rho_k}\right)}=\frac{\hat{\zeta}_k}{\hat{\rho}_k}, \quad (62)$$

(49) can be further simplified. The condition deriving from the first line of the system finally reads

$$\hat{\mathcal{R}}\left(p^{\rm R}-p^{\rm L}\right)=\hat{\alpha}_{\rm g}\hat{\zeta}_\ell\frac{\hat{\zeta}_{\rm g}}{\hat{\rho}_{\rm g}}\left(\rho_{\rm g}^{\rm R}-\rho_{\rm g}^{\rm L}\right)+\hat{\alpha}_\ell\hat{\zeta}_{\rm g}\frac{\hat{\zeta}_\ell}{\hat{\rho}_\ell}\left(\rho_\ell^{\rm R}-\rho_\ell^{\rm L}\right)$$
$$+\breve{\rho}_{\rm g}\hat{\alpha}_{\rm g}\hat{\zeta}_\ell\hat{\Gamma}_{\rm g}\left(e_{\rm g}^{\rm R}-e_{\rm g}^{\rm L}\right)+\breve{\rho}_\ell\hat{\alpha}_\ell\hat{\zeta}_{\rm g}\hat{\Gamma}_\ell\left(e_\ell^{\rm R}-e_\ell^{\rm L}\right). \quad (63)$$

DOI: 10.1002/fld

4.5. Simplification of the second line of the system (46)

The second line of the system (46) reads

$$\begin{aligned}\hat{\mathcal{R}}\left((\alpha_{\mathrm{g}}v_{\mathrm{g}}+\alpha_\ell v_\ell)^{\mathrm{R}}-(\alpha_{\mathrm{g}}v_{\mathrm{g}}+\alpha_\ell v_\ell)^{\mathrm{L}}\right)=&\\ \left((\hat{v}_{\mathrm{g}}-\hat{v}_\ell)\hat{\alpha}_\ell\hat{\beta}_{\mathrm{g}}-\frac{\hat{\mathcal{R}}\hat{v}_{\mathrm{g}}}{\hat{\rho}_{\mathrm{g}}}\right)\left(u_1^{\mathrm{R}}-u_1^{\mathrm{L}}\right)-\left((\hat{v}_{\mathrm{g}}-\hat{v}_\ell)\hat{\alpha}_{\mathrm{g}}\hat{\beta}_\ell-\frac{\hat{\mathcal{R}}\hat{v}_\ell}{\hat{\rho}_\ell}\right)\left(u_2^{\mathrm{R}}-u_2^{\mathrm{L}}\right)&\\ +\left(\frac{\hat{\mathcal{R}}}{\hat{\rho}_{\mathrm{g}}}-(\hat{v}_{\mathrm{g}}-\hat{v}_\ell)\hat{\alpha}_\ell\hat{\Gamma}_{\mathrm{g}}\hat{v}_{\mathrm{g}}\right)\left(u_3^{\mathrm{R}}-u_3^{\mathrm{L}}\right)+\left(\frac{\hat{\mathcal{R}}}{\hat{\rho}_\ell}+(\hat{v}_{\mathrm{g}}-\hat{v}_\ell)\hat{\alpha}_{\mathrm{g}}\hat{\Gamma}_\ell\hat{v}_\ell\right)\left(u_4^{\mathrm{R}}-u_4^{\mathrm{L}}\right)&\\ +(\hat{v}_{\mathrm{g}}-\hat{v}_\ell)\hat{\alpha}_\ell\hat{\Gamma}_{\mathrm{g}}\left(u_5^{\mathrm{R}}-u_5^{\mathrm{L}}\right)-(\hat{v}_{\mathrm{g}}-\hat{v}_\ell)\hat{\alpha}_{\mathrm{g}}\hat{\Gamma}_\ell\left(u_6^{\mathrm{R}}-u_6^{\mathrm{L}}\right).&\quad(64)\end{aligned}$$

This expression will be successively simplified by assuming averaging formulas for the different variables. We first list them. The velocities will follow the same averaging as for the convective part, given by (43). Then, the density Roe-averaging takes the form

$$\hat{\rho}_k=\sqrt{\rho_k^{\mathrm{L}}\rho_k^{\mathrm{R}}}\frac{\sqrt{(\alpha_k\rho_k)^{\mathrm{L}}}+\sqrt{(\alpha_k\rho_k)^{\mathrm{R}}}}{\sqrt{\alpha_k^{\mathrm{L}}\rho_k^{\mathrm{R}}}+\sqrt{\alpha_k^{\mathrm{R}}\rho_k^{\mathrm{L}}}},\tag{65}$$

the volume fraction will be averaged as

$$\hat{\alpha}_k=\frac{\sqrt{\alpha_k^{\mathrm{R}}\rho_k^{\mathrm{L}}}\alpha_k^{\mathrm{L}}+\sqrt{\alpha_k^{\mathrm{L}}\rho_k^{\mathrm{R}}}\alpha_k^{\mathrm{R}}}{\sqrt{\alpha_k^{\mathrm{L}}\rho_k^{\mathrm{R}}}+\sqrt{\alpha_k^{\mathrm{R}}\rho_k^{\mathrm{L}}}},\tag{66}$$

while the internal energy has to have a different form than in the convective part. Its Roe average will be $\tilde{e}$ as defined in (45). Note that the averages (65) and (66) satisfy the relations (57) and (58).

If we assume the velocity Roe-average (43), (64) simplifies to

$$\begin{aligned}\hat{\mathcal{R}}\left((\alpha_{\mathrm{g}}v_{\mathrm{g}})^{\mathrm{R}}-(\alpha_{\mathrm{g}}v_{\mathrm{g}})^{\mathrm{L}}\right)=\hat{v}_{\mathrm{g}}\left(\hat{\alpha}_\ell\left(\widehat{\left(\frac{\zeta_{\mathrm{g}}}{\rho_{\mathrm{g}}}\right)}-\hat{\Gamma}_{\mathrm{g}}\tilde{e}_{\mathrm{g}}\right)-\frac{\hat{\mathcal{R}}}{\hat{\rho}_{\mathrm{g}}}\right)\left(u_1^{\mathrm{R}}-u_1^{\mathrm{L}}\right)&\\ -\hat{\alpha}_{\mathrm{g}}\hat{v}_{\mathrm{g}}\left(\widehat{\left(\frac{\zeta_\ell}{\rho_\ell}\right)}-\hat{\Gamma}_\ell\tilde{e}_\ell\right)\left(u_2^{\mathrm{R}}-u_2^{\mathrm{L}}\right)+\frac{\hat{\mathcal{R}}}{\hat{\rho}_{\mathrm{g}}}\left(u_3^{\mathrm{R}}-u_3^{\mathrm{L}}\right)&\\ +\hat{\alpha}_\ell\hat{\Gamma}_{\mathrm{g}}\hat{v}_{\mathrm{g}}\left((\alpha_{\mathrm{g}}\rho_{\mathrm{g}}e_{\mathrm{g}})^{\mathrm{R}}-(\alpha_{\mathrm{g}}\rho_{\mathrm{g}}e_{\mathrm{g}})^{\mathrm{L}}\right)-\hat{\alpha}_{\mathrm{g}}\hat{\Gamma}_\ell\hat{v}_{\mathrm{g}}\left((\alpha_\ell\rho_\ell e_\ell)^{\mathrm{R}}-(\alpha_\ell\rho_\ell e_\ell)^{\mathrm{L}}\right)&\quad(67)\end{aligned}$$

and

$$\begin{aligned}\hat{\mathcal{R}}\left((\alpha_\ell v_\ell)^{\mathrm{R}}-(\alpha_\ell v_\ell)^{\mathrm{L}}\right)=-\hat{\alpha}_\ell\hat{v}_\ell\left(\widehat{\left(\frac{\zeta_{\mathrm{g}}}{\rho_{\mathrm{g}}}\right)}-\hat{\Gamma}_{\mathrm{g}}\tilde{e}_{\mathrm{g}}\right)\left(u_1^{\mathrm{R}}-u_1^{\mathrm{L}}\right)&\\ +\hat{v}_\ell\left(\hat{\alpha}_{\mathrm{g}}\left(\widehat{\left(\frac{\zeta_\ell}{\rho_\ell}\right)}-\hat{\Gamma}_\ell\tilde{e}_\ell\right)-\frac{\hat{\mathcal{R}}}{\hat{\rho}_\ell}\right)\left(u_2^{\mathrm{R}}-u_2^{\mathrm{L}}\right)+\frac{\hat{\mathcal{R}}}{\hat{\rho}_\ell}\left(u_4^{\mathrm{R}}-u_4^{\mathrm{L}}\right)&\\ -\hat{\alpha}_\ell\hat{\Gamma}_{\mathrm{g}}\hat{v}_\ell\left((\alpha_{\mathrm{g}}\rho_{\mathrm{g}}e_{\mathrm{g}})^{\mathrm{R}}-(\alpha_{\mathrm{g}}\rho_{\mathrm{g}}e_{\mathrm{g}})^{\mathrm{L}}\right)+\hat{\alpha}_{\mathrm{g}}\hat{\Gamma}_\ell\hat{v}_\ell\left((\alpha_\ell\rho_\ell e_\ell)^{\mathrm{R}}-(\alpha_\ell\rho_\ell e_\ell)^{\mathrm{L}}\right).&\quad(68)\end{aligned}$$

Proof

The above conditions (67)–(68) are summed, and the right-hand side of the resulting expression is equated to that of the condition (64). This results in the two conditions already found for the convective part (55)–(56), and they are satisfied for the velocity averaging formula (43). □

DOI: 10.1002/fld

4.6. Density average

Then, if we assume a density average of the form (65), the conditions (67)–(68) reduce to

$$\hat{\mathcal{R}}\left((\alpha_\mathrm{g})^\mathrm{R}-(\alpha_\mathrm{g})^\mathrm{L}\right)=\hat{\alpha}_\ell\left(\widehat{\left(\frac{\zeta_\mathrm{g}}{\rho_\mathrm{g}}\right)}-\hat{\Gamma}_\mathrm{g}\tilde{e}_\mathrm{g}\right)\left(u_1^\mathrm{R}-u_1^\mathrm{L}\right)-\hat{\alpha}_\mathrm{g}\left(\widehat{\left(\frac{\zeta_\ell}{\rho_\ell}\right)}-\hat{\Gamma}_\ell\tilde{e}_\ell\right)\left(u_2^\mathrm{R}-u_2^\mathrm{L}\right)$$
$$+\hat{\alpha}_\ell\hat{\Gamma}_\mathrm{g}\left((\alpha_\mathrm{g}\rho_\mathrm{g}e_\mathrm{g})^\mathrm{R}-(\alpha_\mathrm{g}\rho_\mathrm{g}e_\mathrm{g})^\mathrm{L}\right)-\hat{\alpha}_\mathrm{g}\hat{\Gamma}_\ell\left((\alpha_\ell\rho_\ell e_\ell)^\mathrm{R}-(\alpha_\ell\rho_\ell e_\ell)^\mathrm{L}\right). \quad (69)$$

Proof
First, observe that

$$(\alpha_k v_k)^\mathrm{R}-(\alpha_k v_k)^\mathrm{L}=\check{\alpha}_k\left(v_k^\mathrm{R}-v_k^\mathrm{L}\right)+\hat{v}_k\left(\alpha_k^\mathrm{R}-\alpha_k^\mathrm{L}\right) \quad (70)$$

where $\hat{v}_k$ is given by (43), $\hat{\rho}_k$ by (65) and

$$\check{\alpha}_k=\frac{\sqrt{(\alpha_k\rho_k)^\mathrm{R}}\alpha_k^\mathrm{L}+\sqrt{(\alpha_k\rho_k)^\mathrm{L}}\alpha_k^\mathrm{R}}{\sqrt{(\alpha_k\rho_k)^\mathrm{L}}+\sqrt{(\alpha_k\rho_k)^\mathrm{R}}}. \quad (71)$$

These averaging formulas also satisfy

$$\check{\alpha}_\mathrm{g}\left(v_\mathrm{g}^\mathrm{R}-v_\mathrm{g}^\mathrm{L}\right)=-\frac{\hat{v}_\mathrm{g}}{\hat{\rho}_\mathrm{g}}\left(u_1^\mathrm{R}-u_1^\mathrm{L}\right)+\frac{1}{\hat{\rho}_\mathrm{g}}\left(u_3^\mathrm{R}-u_3^\mathrm{L}\right) \quad (72)$$

$$\check{\alpha}_\ell\left(v_\ell^\mathrm{R}-v_\ell^\mathrm{L}\right)=-\frac{\hat{v}_\ell}{\hat{\rho}_\ell}\left(u_2^\mathrm{R}-u_2^\mathrm{L}\right)+\frac{1}{\hat{\rho}_\ell}\left(u_4^\mathrm{R}-u_4^\mathrm{L}\right). \quad (73)$$

Now, write (70) for phases g and ℓ, substitute into them respectively (72) and (73), and substitute them in turn respectively into (67) and (68). Since $\alpha_\mathrm{g}+\alpha_\ell=1$, both expression reduce to (69). □

4.7. Internal energy average for the pressure part

Finally, if we assume that the volume fraction average follows (66) and the internal energy average follows the form of $\tilde{e}$ in (45), the condition (69) can be written as

$$\widehat{\left(\frac{\zeta_\mathrm{g}}{\rho_\mathrm{g}}\right)}\left(\rho_\mathrm{g}^\mathrm{R}-\rho_\mathrm{g}^\mathrm{L}\right)-\widehat{\left(\frac{\zeta_\ell}{\rho_\ell}\right)}\left(\rho_\ell^\mathrm{R}-\rho_\ell^\mathrm{L}\right)+\check{\rho}_\mathrm{g}\hat{\Gamma}_\mathrm{g}\left(e_\mathrm{g}^\mathrm{R}-e_\mathrm{g}^\mathrm{L}\right)-\check{\rho}_\ell\hat{\Gamma}_\ell\left(e_\ell^\mathrm{R}-e_\ell^\mathrm{L}\right)=0, \quad (74)$$

where we have used the shorthand (61).

Proof
Recall the expressions (57), (58) and (60). Substituting them into (69), using (66) and (45) as averaging formulas, as well as defining

$$\hat{\mathcal{R}}=\hat{\alpha}_\mathrm{g}\hat{\zeta}_\ell+\hat{\alpha}_\ell\hat{\zeta}_\mathrm{g} \quad (75)$$

yields the result after cancelling the equal terms. □

4.8. A relation for the pressure average

We have now reduced the two first lines of the system resulting from the pressure part of the Roe condition to the expressions (63) and (74). With the definitions of the averages (43), (45), (65) and (66) as well as the definitions (62) and (75), they can be recombined as

$$p^\mathrm{R}-p^\mathrm{L}=\frac{\hat{\zeta}_\mathrm{g}}{\hat{\rho}_\mathrm{g}}\left(\rho_\mathrm{g}^\mathrm{R}-\rho_\mathrm{g}^\mathrm{L}\right)+\check{\rho}_\mathrm{g}\hat{\Gamma}_\mathrm{g}\left(e_\mathrm{g}^\mathrm{R}-e_\mathrm{g}^\mathrm{L}\right) \quad (76)$$

$$=\frac{\hat{\zeta}_\ell}{\hat{\rho}_\ell}\left(\rho_\ell^\mathrm{R}-\rho_\ell^\mathrm{L}\right)+\check{\rho}_\ell\hat{\Gamma}_\ell\left(e_\ell^\mathrm{R}-e_\ell^\mathrm{L}\right). \quad (77)$$

This resembles a Roe average of the differential (17).

DOI: 10.1002/fld

4.9. Simplification of the third line of the system (46)

The third line of the system (46) reads

$$\hat{\mathcal{R}}\left(\alpha_{\mathrm{g}}^{\mathrm{R}}-\alpha_{\mathrm{g}}^{\mathrm{L}}\right)=\hat{\alpha}_{\ell}\hat{\beta}_{\mathrm{g}}\left(u_{1}^{\mathrm{R}}-u_{1}^{\mathrm{L}}\right)-\hat{\alpha}_{\mathrm{g}}\hat{\beta}_{\ell}\left(u_{2}^{\mathrm{R}}-u_{2}^{\mathrm{L}}\right)$$
$$-\hat{\alpha}_{\ell}\hat{\Gamma}_{\mathrm{g}}\hat{v}_{\mathrm{g}}\left(u_{3}^{\mathrm{R}}-u_{3}^{\mathrm{L}}\right)+\hat{\alpha}_{\mathrm{g}}\hat{\Gamma}_{\ell}\hat{v}_{\ell}\left(u_{4}^{\mathrm{R}}-u_{4}^{\mathrm{L}}\right)+\hat{\alpha}_{\ell}\hat{\Gamma}_{\mathrm{g}}\left(u_{5}^{\mathrm{R}}-u_{5}^{\mathrm{L}}\right)-\hat{\alpha}_{\mathrm{g}}\hat{\Gamma}_{\ell}\left(u_{6}^{\mathrm{R}}-u_{6}^{\mathrm{L}}\right),\quad(78)$$

where $\hat{\beta}_k$ is given by (48) and $\hat{\mathcal{R}}$ is as defined in (75).

Now, if the velocities are averaged following the formula (43), the condition (78) reduces to

$$\hat{\mathcal{R}}\left(\alpha_{\mathrm{g}}^{\mathrm{R}}-\alpha_{\mathrm{g}}^{\mathrm{L}}\right)=$$
$$\hat{\alpha}_{\ell}\left(\frac{\hat{\zeta}_{\mathrm{g}}}{\hat{\rho}_{\mathrm{g}}}-\hat{\Gamma}_{\mathrm{g}}\tilde{e}_{\mathrm{g}}\right)\left((\alpha_{\mathrm{g}}\rho_{\mathrm{g}})^{\mathrm{R}}-(\alpha_{\mathrm{g}}\rho_{\mathrm{g}})^{\mathrm{L}}\right)-\hat{\alpha}_{\mathrm{g}}\left(\frac{\hat{\zeta}_{\ell}}{\hat{\rho}_{\ell}}-\hat{\Gamma}_{\ell}\tilde{e}_{\ell}\right)\left((\alpha_{\ell}\rho_{\ell})^{\mathrm{R}}-(\alpha_{\ell}\rho_{\ell})^{\mathrm{L}}\right)$$
$$+\hat{\alpha}_{\ell}\hat{\Gamma}_{\mathrm{g}}\left((\alpha_{\mathrm{g}}\rho_{\mathrm{g}}e_{\mathrm{g}})^{\mathrm{R}}-(\alpha_{\mathrm{g}}\rho_{\mathrm{g}}e_{\mathrm{g}})^{\mathrm{L}}\right)-\hat{\alpha}_{\mathrm{g}}\hat{\Gamma}_{\ell}\left((\alpha_{\ell}\rho_{\ell}e_{\ell})^{\mathrm{R}}-(\alpha_{\ell}\rho_{\ell}e_{\ell})^{\mathrm{L}}\right),\quad(79)$$

Proof
Equating the right-hand sides of the expression (78) and (79) yields

$$\frac{1}{2}\hat{\alpha}_{\ell}\hat{\Gamma}_{\mathrm{g}}\hat{v}_{\mathrm{g}}^{2}\left((\alpha_{\mathrm{g}}\rho_{\mathrm{g}})^{\mathrm{R}}-(\alpha_{\mathrm{g}}\rho_{\mathrm{g}})^{\mathrm{L}}\right)-\frac{1}{2}\hat{\alpha}_{\mathrm{g}}\hat{\Gamma}_{\ell}\hat{v}_{\ell}\left((\alpha_{\ell}\rho_{\ell})^{\mathrm{R}}-(\alpha_{\ell}\rho_{\ell})^{\mathrm{L}}\right)$$
$$-\hat{\alpha}_{\ell}\hat{\Gamma}_{\mathrm{g}}\hat{v}_{\mathrm{g}}\left((\alpha_{\mathrm{g}}\rho_{\mathrm{g}}v_{\mathrm{g}})^{\mathrm{R}}-(\alpha_{\mathrm{g}}\rho_{\mathrm{g}}v_{\mathrm{g}})^{\mathrm{L}}\right)+\hat{\alpha}_{\mathrm{g}}\hat{\Gamma}_{\ell}\hat{v}_{\ell}\left((\alpha_{\ell}\rho_{\ell}v_{\ell})^{\mathrm{R}}-(\alpha_{\ell}\rho_{\ell}v_{\ell})^{\mathrm{L}}\right)$$
$$+\frac{1}{2}\hat{\alpha}_{\ell}\hat{\Gamma}_{\mathrm{g}}\left((\alpha_{\mathrm{g}}\rho_{\mathrm{g}}v_{\mathrm{g}}^{2})^{\mathrm{R}}-(\alpha_{\mathrm{g}}\rho_{\mathrm{g}}v_{\mathrm{g}}^{2})^{\mathrm{L}}\right)-\frac{1}{2}\hat{\alpha}_{\mathrm{g}}\hat{\Gamma}_{\ell}\left((\alpha_{\ell}\rho_{\ell}v_{\ell}^{2})^{\mathrm{R}}-(\alpha_{\ell}\rho_{\ell}v_{\ell}^{2})^{\mathrm{L}}\right)=0,\quad(80)$$

which is satisfied by the averaging formula (43). □

Finally, if we assume that the averaging formulas for the volume fraction $\hat{\alpha}$ (66), the density $\hat{\rho}$ (65) and the internal energy $\tilde{e}$ (45) hold, the condition (79) simplifies to

$$\frac{\hat{\zeta}_{\mathrm{g}}}{\hat{\rho}_{\mathrm{g}}}\left(\rho_{\mathrm{g}}^{\mathrm{R}}-\rho_{\mathrm{g}}^{\mathrm{L}}\right)-\frac{\hat{\zeta}_{\ell}}{\hat{\rho}_{\ell}}\left(\rho_{\ell}^{\mathrm{R}}-\rho_{\ell}^{\mathrm{L}}\right)+\breve{\rho}_{\mathrm{g}}\hat{\Gamma}_{\mathrm{g}}\left(e_{\mathrm{g}}^{\mathrm{R}}-e_{\mathrm{g}}^{\mathrm{L}}\right)-\breve{\rho}_{\ell}\hat{\Gamma}_{\ell}\left(e_{\ell}^{\mathrm{R}}-e_{\ell}^{\mathrm{L}}\right)=0.\quad(81)$$

Proof
Using the relations (57) and (58), the expression (79) can be written as

$$\left(\frac{\hat{\zeta}_{\mathrm{g}}}{\hat{\rho}_{\mathrm{g}}}-\hat{\Gamma}_{\mathrm{g}}\tilde{e}_{\mathrm{g}}\right)\left(\rho_{\mathrm{g}}^{\mathrm{R}}-\rho_{\mathrm{g}}^{\mathrm{L}}\right)-\left(\frac{\hat{\zeta}_{\ell}}{\hat{\rho}_{\ell}}-\hat{\Gamma}_{\ell}\tilde{e}_{\ell}\right)\left(\rho_{\ell}^{\mathrm{R}}-\rho_{\ell}^{\mathrm{L}}\right)$$
$$+\hat{\Gamma}_{\mathrm{g}}\left((\rho_{\mathrm{g}}e_{\mathrm{g}})^{\mathrm{R}}-(\rho_{\mathrm{g}}e_{\mathrm{g}})^{\mathrm{L}}\right)-\hat{\Gamma}_{\ell}\left((\rho_{\ell}e_{\ell})^{\mathrm{R}}-(\rho_{\ell}e_{\ell})^{\mathrm{L}}\right)=0.\quad(82)$$

The expression (81) follows from using the relation (60). □

The relation (81) is satisfied whenever the relations resulting from the two first lines (76) and (77) are satisfied.

4.10. Remaining variables

The last variables in the conditions (76) and (77) for which we did not define a Roe average are ζ_k and Γ_k. Recall the definition $\zeta_k=\rho_k c_k^2-\Gamma_k p$. It is dependent on the equation of state because the speed of sound c and Γ are thermodynamical parameters. Therefore the remaining averaging formulas cannot be deduced analytically from these conditions without specifying the equation of state. On the other hand, there exist approaches to construct the required averages numerically, when the equation of state is in the form of a "black box"

DOI: 10.1002/fld

(see for example the approach presented in [29]). This is an advantage when using tabulated equations of state.

Note that the internal energy averages for the convective part (44) and the pressure part (45) are different from each other. Hence the full matrix cannot in general be written in the form

$$\hat{\boldsymbol{A}}(\boldsymbol{U}^{\mathrm{L}},\boldsymbol{U}^{\mathrm{R}}) = \boldsymbol{A}(\hat{\boldsymbol{U}}(\boldsymbol{U}^{\mathrm{L}},\boldsymbol{U}^{\mathrm{R}})). \tag{83}$$

In addition, in general

$$\hat{\alpha}_{\mathrm{g}} + \hat{\alpha}_{\ell} \neq 1. \tag{84}$$

However, this is just a feature of the formulation of the averaging and does not in any way affect the numerical consistency of the scheme. In particular, the conditions R2 and R3 are unconditionally satisfied. The condition R1 holds only conditionally for the model itself, and is discussed in more detail in Section 6.

4.11. Application to stiffened gas

The derivation above was independent of the choice of equation of state. For the purpose of numerical testing in the present work, we have used the stiffened gas equation of state. This equation of state is based on the ideal gas law, to which a factor is added to reduce the compressibility. It can then represent liquid-like fluids in addition to gases. It is expressed by

$$p(\rho,T) = \frac{\gamma-1}{\gamma}\rho C_p T - p_\infty \tag{85}$$

$$e(\rho,T) = \frac{C_p}{\gamma}T + \frac{p_\infty}{\rho}. \tag{86}$$

where γ, p_∞ and C_p are constants.

To represent a two-phase flow of a liquid and a gas at mechanical equilibrium, we then define two fluids following the equation of state (85)–(86), sharing the same pressure and whose volume fractions sum to one. To evaluate the state of the two fluids from the vector of conserved variables, we use in the present work the algorithm described in [30].

With the choice of an equation of state, we are now able to define Roe averages for ζ_k and Γ_k. First, we can write

$$p = \Gamma_k \rho_k e_k - \gamma_k p_\infty, \tag{87}$$

where Γ is the first Grüneisen coefficient, which for the stiffened gas equation of state is $\Gamma = \gamma - 1$. This gives

$$\mathrm{d}p = \Gamma_k \,\mathrm{d}(\rho_k e_k) = \Gamma_k e_k \,\mathrm{d}\rho_k + \Gamma_k \rho_k \,\mathrm{d}e_k. \tag{88}$$

By comparison with the differential (17), we deduce

$$\zeta_k = \Gamma_k e_k \rho_k. \tag{89}$$

We choose to define the averages as

$$\hat{\Gamma}_k = \Gamma_k, \tag{90}$$

and

$$\hat{\zeta}_k = \Gamma_k \breve{e}_k \hat{\rho}_k. \tag{91}$$

We now need to define the average $\breve{e}_k$ in order to satisfy the Roe condition (42). From (76)–(77) and (87), we obtain

$$p^{\mathrm{R}} - p^{\mathrm{L}} = \Gamma_k(\rho_k^{\mathrm{R}} e_k^{\mathrm{R}} - \rho_k^{\mathrm{L}} e_k^{\mathrm{L}}) = \frac{\Gamma_k \breve{e}_k \hat{\rho}_k}{\hat{\rho}_k}(\rho_k^{\mathrm{R}} - \rho_k^{\mathrm{L}}) + \breve{\rho}_k \Gamma_k (e_k^{\mathrm{R}} - e_k^{\mathrm{L}}) \tag{92}$$

DOI: 10.1002/fld

which simplifies to

$$\rho_k^{\mathrm{R}} e_k^{\mathrm{R}} - \rho_k^{\mathrm{L}} e_k^{\mathrm{L}} = \frac{\breve{e}_k \hat{\rho}_k}{\hat{\rho}_k}(\rho_k^{\mathrm{R}} - \rho_k^{\mathrm{L}}) + \breve{\rho}_k(e_k^{\mathrm{R}} - e_k^{\mathrm{L}}) \tag{93}$$

which is verified by the definition (61) and the internal energy average (45)

$$\breve{e}_k = \frac{\sqrt{\alpha_k^{\mathrm{L}}\rho_k^{\mathrm{L}}}e_k^{\mathrm{L}} + \sqrt{\alpha_k^{\mathrm{R}}\rho_k^{\mathrm{R}}}e_k^{\mathrm{R}}}{\sqrt{\alpha_k^{\mathrm{L}}\rho_k^{\mathrm{L}}} + \sqrt{\alpha_k^{\mathrm{R}}\rho_k^{\mathrm{R}}}} = \tilde{e}_k. \tag{94}$$

Note that with the stiffened gas equation of state, the Roe average of the pressure is not used.

5. NON-CONSERVATIVE TERMS

In the *formally path-conservative* framework [10], the non-conservative terms are integrated between the left and right states along a given path, giving the averaging formulas for the non-conservative factors gathered in the matrix $\boldsymbol{B}$. Some previous works pointed out that this approach may converge to a weak solution with the wrong shock speeds [15, 16]. Other approaches to handle non-conservative terms consist in flux splitting, see for example [4]. In these approaches, the solution is advanced one time step with the conservative fluxes, before the non-conservative terms are applied as source terms. Therefore the whole wave structure is not captured during the conservative time step. This results in smearing of the discontinuities. By letting the non-conservative terms affect the wave structure of the model, this smearing is avoided. The *formally path-conservative* framework allows that, since all the differential terms are solved at the same time. Further, this is an advantage for the purpose of analysis since we have access, at least numerically, to the real velocity of the waves.

Choosing the right integration path for the matrix $\boldsymbol{B}$ is not the object of this article. As shown with (46), the matrix $\boldsymbol{B}$ disappears from the Roe condition. Therefore the choice of the path does not interact with the derivation of the Roe averages, and the Roe scheme here presented is independent of the choice of path. However, it has been observed that if the $\boldsymbol{B}$-averages are too different from the Roe averages, the resulting matrix $\boldsymbol{A}$ may have complex eigenvalues. Now, in [2], it was shown that the averaging method for the matrix $\boldsymbol{B}$ has limited effect on the results for Toumi's shock tube with the six-equation system. Therefore, we found it convenient to choose the Roe averages for evaluating the matrix $\boldsymbol{B}$. The pressure can have a particular treatment. Since we have used the stiffened gas equation of state, the Roe average of the pressure is not used (cf. Section 4.11). This average generally has to be found numerically using the relations (76)–(77). We have here simply used the arithmetic average for the pressure in the matrix $\boldsymbol{B}$.

Note that our scheme can only be said to be implicitly path-consistent, as the existence of a definite path corresponding to these averages is here an a priori assumption. In this respect, we follow the approach of [2]. Nevertheless, our method will be *formally path-consistent* for any path giving the $\boldsymbol{B}$-averaging employed in this paper.

6. RESONANCE OF THE SYSTEM

When the velocities are equal to each other, the Jacobian matrix $\boldsymbol{A}$ (40) is not diagonalisable. The system is then said to be resonant. Since the Roe scheme is based on diagonalising this matrix, this seriously impairs the robustness of the method.

DOI: 10.1002/fld

6.1. Collapse of the eigenspace

The two-fluid model has six eigenvalues. Two of them correspond to the speed of the pressure waves in both directions, two others correspond to the speed of the interfacial waves – also called volume-fraction waves – in both directions. The last two correspond to the convection speed of the entropy in each phase. Only the last two are known analytically: v_g and v_ℓ. Otherwise, the eigenstructure of the two-fluid model is in general not known. However, when $v_\mathrm{g} = v_\ell$, we are able to obtain general analytical eigenvalues and eigenvectors for the entropy and volume-fraction waves. If we substitute v_m for v_g and v_ℓ in the matrix $\boldsymbol{A}$ (40), v_m is an eigenvalue with multiplicity four. The corresponding eigenvector can be shown to be

$$\boldsymbol{X}_{v_\mathrm{m}} = \begin{bmatrix} \omega_1 \\ \omega_2 \\ v_\mathrm{m}\omega_1 \\ v_\mathrm{m}\omega_2 \\ \frac{1}{2}v_\mathrm{m}^2\omega_1 - e_\mathrm{g}\rho_\mathrm{g}\omega_3 \\ \frac{1}{2}v_\mathrm{m}^2\omega_2 + e_\ell\rho_\ell\omega_3 \end{bmatrix}. \tag{95}$$

This vector only contains three degrees of freedom $(\omega_1, \omega_2, \omega_3)$, which is less than the multiplicity of the eigenvalue. This shows that the matrix is not diagonalisable. When $v_\mathrm{g} \neq v_\ell$, however, the eigenvalues become generally distinct, and so do the eigenvectors. In particular, the eigenvectors corresponding to the eigenvalues v_g and v_ℓ are respectively

$$\boldsymbol{X}_{v_\mathrm{g}} = \begin{bmatrix} 1 \\ 0 \\ v_\mathrm{g} \\ 0 \\ \frac{1}{2}v_\mathrm{g}^2 \\ 0 \end{bmatrix} \qquad \text{and} \qquad \boldsymbol{X}_{v_\ell} = \begin{bmatrix} 0 \\ 1 \\ 0 \\ v_\ell \\ 0 \\ \frac{1}{2}v_\ell^2 \end{bmatrix}. \tag{96}$$

These vectors describe the entropy waves, propagating at the velocity of the phases. We can remark that when $(v_\mathrm{g}, v_\ell) \to (v_\mathrm{m}, v_\mathrm{m})$

$$\boldsymbol{X}_{v_\mathrm{m}} = \omega_1 \boldsymbol{X}_{v_\mathrm{g}}(v_\mathrm{g} = v_\mathrm{m}) + \omega_2 \boldsymbol{X}_{v_\ell}(v_\ell = v_\mathrm{m}) + \omega_3 \begin{bmatrix} 0 \\ 0 \\ 0 \\ 0 \\ -e_\mathrm{g}\rho_\mathrm{g} \\ e_\ell\rho_\ell \end{bmatrix}. \tag{97}$$

Both eigenvectors describing the entropy waves are independent and present in $\boldsymbol{X}_{v_\mathrm{m}}$, while only one dimension remains for the vectors describing the volume-fraction waves. We deduce that the eigenspace collapsing is the one associated with the volume-fraction waves. Those waves do indeed become identical when they propagate at identical velocities, therefore their corresponding eigenvectors cross each other at $v_\mathrm{g} = v_\ell$. Note that this is a purely mathematical phenomenon, not a physical one. The eigenspace collapses because the waves become identical, such that their eigenvectors become equal. Physically, both waves are still present, but superimposed. This is why resonance is not a problem for the MUSTA method [2], which does not use the eigenstructure of the model.

6.2. Correction of the numerical scheme

This results in the Roe scheme being inapplicable when $|v_\mathrm{g} - v_\ell| < \varepsilon$ (ε being a small quantity depending on the machine precision) because the vectors will be indistinct at machine precision. To overcome this difficulty, we will take advantage of the continuity of the eigenvectors with respect to $v_\mathrm{g} - v_\ell$.

DOI: 10.1002/fld

For some small ε, for each interface where the averaged state is such that $|v_\mathrm{g} - v_\ell| < \varepsilon$, we apply the following procedure. For an interface between the cell i and $i+1$, the velocities are modified as follows

$$v_\mathrm{g}^i \to v_\mathrm{g}^i + \varepsilon \qquad v_\mathrm{g}^{i+1} \to v_\mathrm{g}^{i+1} + \varepsilon \tag{98}$$

$$v_\ell^i \to v_\ell^i - \varepsilon \qquad v_\ell^{i+1} \to v_\ell^{i+1} - \varepsilon, \tag{99}$$

before the Roe fluctuations (cf. [31], p. 80) are evaluated at the interface for these states. Then the velocities are again modified as

$$v_\mathrm{g}^i \to v_\mathrm{g}^i - \varepsilon \qquad v_\mathrm{g}^{i+1} \to v_\mathrm{g}^{i+1} - \varepsilon \tag{100}$$

$$v_\ell^i \to v_\ell^i + \varepsilon \qquad v_\ell^{i+1} \to v_\ell^{i+1} + \varepsilon. \tag{101}$$

The Roe fluctuations are also evaluated for these states. Then the approximate fluctuations with the original velocities are obtained by taking the arithmetic average.

6.3. Effect of the regularisation of the model

The regularisation term Δp used in this work vanishes when $v_\mathrm{g} = v_\ell$, and resonance occurs. Now, theoretically, if the pressure difference between the phases is not zero when $v_\mathrm{g} = v_\ell$, resonance should be avoided. This is because the eigenvalues associated with volume fraction waves then are slightly different from each other. However, physically sensible regularisation terms will generally give small pressure differences compared to the phase pressures. To investigate whether this is enough to avoid the resonance problems, we added to our regularisation term Δp a term in the form proposed by Soo [32] (pp. 319–321), $C \cdot p$, where p is the pressure, and C is a constant. These investigations showed a strong loss of numerical accuracy in the proximity of the state $v_\mathrm{g} = v_\ell$, even when the system would theoretically not be resonant for the volume-fraction waves. This is due to the eigenvectors matrix being badly conditioned. A constant C of the order of unity – thus Δp of the order of the fluid pressure – was necessary in order to be able to run the scheme without the resonance fix exposed in the previous section. This is not physical, therefore the fix is also necessary with any physically meaningful pressure difference Δp between the phases.

7. SECOND ORDER SCHEME WITH WAVE LIMITERS

The Roe scheme presented so far is first order. It can be made second order by using the MUSCL [33] reconstruction of the data, along with e.g. a second-order Runge-Kutta solver for the time integration. However, a specific second-order extension of the Roe scheme exists, that does not require several stages in the time integration, thus saving computational time. It is the wave-limiter approach described in the book of LeVeque [31] (pp. 181–183). This method consists in comparing the waves at an interface with the corresponding upwind waves. The wave $\boldsymbol{\omega}_{i-1/2}^p$, of family p and at the interface where the flux is to be evaluated $(i-1/2)$, is defined by

$$\boldsymbol{\omega}_{i-1/2}^p = \left(\ell_{i-1/2}^p \Delta \boldsymbol{U}_{i-1/2}\right) r_{i-1/2}^p, \tag{102}$$

where $\ell_{i-1/2}^p$ and $r_{i-1/2}^p$ are the respectively left and right eigenvectors corresponding to the p^{th} eigenvalue of the Riemann problem at interface $i-1/2$. $\Delta \boldsymbol{U}_{i-1/2}$ is the jump at interface $i-1/2$. At the upwind interface, the wave is defined by

$$\boldsymbol{\omega}_{I-1/2}^p = \left(\ell_{I-1/2}^p \Delta \boldsymbol{U}_{I-1/2}\right) r_{I-1/2}^p, \tag{103}$$

where $I \in [i-1, i+1]$ selects the adjacent interface in the upwind direction. Whether the upwind interface is the left or the right one depends on the sign of the p^{th} eigenvalue. Then

Prepared using fldauth.cls
DOI: 10.1002/fld

a smoothness measure is evaluated, similar to the slope ratio in the MUSCL approach, in order to construct a wave correction. The smoothness measure for wave p is defined by

$$\theta^p_{i-1/2} = \frac{\boldsymbol{\omega}^p_{I-1/2} \cdot \boldsymbol{\omega}^p_{i-1/2}}{\boldsymbol{\omega}^p_{i-1/2} \cdot \boldsymbol{\omega}^p_{i-1/2}}. \tag{104}$$

The drawback of this method is that it is dependent on the ordering of the eigenvalues, because the definition of the upwind wave $\boldsymbol{\omega}^p_{I-1/2}$ uses the eigenstructure of the Riemann problem at the upwind interface $I-1/2$. To employ (104), one needs to know which wave the index p actually represents. For the two-fluid model, the eigenvalues must be calculated numerically, and we have in general no method of determining which eigenvalue belongs to which family of waves. Hence the above method is not directly applicable, for it will fail each time the eigenvalues change order from an interface to the next. Instead, Lax and Liu [34] defined a new smoothness measure, where the information coming from adjacent cells only comes from the jump $\Delta \boldsymbol{U}_{I-1/2}$, which is independent of the wave ordering. The upwind wave is now defined as

$$\widehat{\boldsymbol{\omega}}^p_{I-1/2} = \left(\ell^p_{i-1/2} \Delta \boldsymbol{U}_{I-1/2}\right) r^p_{i-1/2}. \tag{105}$$

Remark that only the eigenvectors at interface $i-1/2$ are used. The smoothness measure is now defined as

$$\theta^p_{i-1/2} = \frac{\widehat{\boldsymbol{\omega}}^p_{I-1/2} \cdot \boldsymbol{\omega}^p_{i-1/2}}{\boldsymbol{\omega}^p_{i-1/2} \cdot \boldsymbol{\omega}^p_{i-1/2}}. \tag{106}$$

This smoothness measure is however a less precise measure of the variation in the wave, since it decomposes the jump $\Delta \boldsymbol{U}_{I-1/2}$ at the upwind interface using the eigenvectors of the Riemann problem at interface $i-1/2$. This can in some cases produce an oscillation in the solution, as will be discussed in the numerical results.

A limited version of the wave is then defined as [31, p. 182]

$$\tilde{\boldsymbol{\omega}}^p_{i-1/2} = \phi(\theta^p_{i-1/2}) \widehat{\boldsymbol{\omega}}^p_{i-1/2}, \tag{107}$$

where $\phi(\theta)$ is the limiter function, which is used to evaluate the limited flux

$$\tilde{\boldsymbol{F}}_{i-1/2} = \frac{1}{2} \sum_{p=1}^{m} |s^p_{i-1/2}| \left(1 - \frac{\Delta t}{\Delta x} |s^p_{i-1/2}|\right) \tilde{\boldsymbol{\omega}}^p_{i-1/2}. \tag{108}$$

The scheme with the second-order extension then reads

$$\boldsymbol{U}^{n+1}_i = \boldsymbol{U}^n_i - \frac{\Delta t}{\Delta x} \left(\mathcal{A}^- \Delta \boldsymbol{U}_{i+1/2} + \mathcal{A}^+ \Delta \boldsymbol{U}_{i-1/2}\right) - \frac{\Delta t}{\Delta x} \left(\tilde{\boldsymbol{F}}_{i+1/2} - \tilde{\boldsymbol{F}}_{i-1/2}\right), \tag{109}$$

where the fluctuations $\mathcal{A}^{\pm} \Delta \boldsymbol{U}_{i-1/2}$ and the wave velocities $s^p_{i-1/2}$ are those of the classical Roe scheme, defined in [31, p. 120].

8. NUMERICAL RESULTS

Some tests have been run on the six-equation two-fluid model using the presently described Roe scheme. Since some of the waves can have a zero velocity, an entropy fix is needed. Harten's entropy fix [31] (p. 324) with $\delta_{\text{Hart}} = 20$ is therefore active on all the test cases. Note that the MUSTA method does not require an entropy fix. The thermodynamical parameters used in the stiffened gas equation of state (85)–(86) are listed in Table II.

Prepared using fldauth.cls
DOI: 10.1002/fld

Table II. Thermodynamical parameters for the stiffened gas equation of state.

	Gas (g)	Liquid (ℓ)
$\gamma\,(-)$	1.4	2.8
p_∞ (Pa)	0.0	8.5×10^8
C_p (J/(kg.K))	1008.7	4186.0

8.1. Isolated waves

Castro *et al.* [15] and Abgrall and Karni [16] write that formally path-consistent schemes may feature slightly wrong wave velocities, compared to the wave velocities predicted by the Rankine-Hugoniot system for a given averaging of $\overline{\boldsymbol{B}}$. In the present section, we test the Rankine-Hugoniot system on each of the six waves occurring in the two-fluid six-equation model. All the tests start with the same left state, given in Table X in Appendix A. The six right states were produced by numerically browsing the Rankine-Hugoniot system

$$\sigma\left(\boldsymbol{U}^R-\boldsymbol{U}^L\right)=\hat{\boldsymbol{A}}\left(\boldsymbol{U}^L,\boldsymbol{U}^R\right)\left(\boldsymbol{U}^R-\boldsymbol{U}^L\right). \tag{110}$$

When relevant, a shock has been chosen rather than a rarefaction. The right states can be found from $\Delta\boldsymbol{U}$ listed in Table XI in Appendix A through

$$\boldsymbol{U}_R=\boldsymbol{U}_L+\Delta\boldsymbol{U}. \tag{111}$$

The waves are numbered by increasing order of velocity. Waves 1 and 6 are the pressure waves, waves 2 and 4 are the volume fraction waves and waves 3 and 5 are the entropy waves.

The waves propagate in a domain of 10,000 cells, and are located at $t=0\,\mathrm{s}$ either at cell 100 for the right-going waves, or at cell 900 for the left-going waves. The simulation time is determined so that the wave travels to the other end of the tube. The minmod wave limiter is used and the CFL number is 0.5. $\delta=2$ was used in the regularisation term (10). To evaluate the propagation velocity, the location of the waves is estimated to be at the inflexion point of $u_1=\alpha_\mathrm{g}\rho_\mathrm{g}$ (or $u_2=\alpha_\ell\rho_\ell$ when $u_1=\alpha_\mathrm{g}\rho_\mathrm{g}$ is constant).

The Rankine-Hugoniot condition is tested by evaluating the two sides of the Rankine-Hugoniot system (110): $\sigma\Delta\boldsymbol{U}$ and $\hat{\boldsymbol{A}}\cdot\Delta\boldsymbol{U}$. The measured wave velocity σ and the relative error of the two sides of the system for each wave type is reported in Table III. When one of the sides was a zero, the relative error has been replaced by an absolute error, denoted by (abs.) in the result table.

We can see that the relative error is most of the time on the order of 10^{-5} or lower, and that it is very similar for all variables. This indicates that this small error comes from the wave velocity σ, but that the jump satisfies the Rankine-Hugoniot system rather strictly. The error in the wave velocity σ may be explained either by the uncertainty in locating the waves, or by a slightly wrong propagation velocity. The exception is wave 2. The relative error goes up to 10^{-3} for the momentum components, and is not homogeneous for all the variables. This indicates that the jump in itself slightly violates the Rankine-Hugoniot condition. This phenomenon seems similar to what was observed in [16], though here in a much smaller scale.

This test shows that the wave velocities and jumps satisfy the Rankine-Hugoniot condition reasonably well in the conditions presented here. However, the error may be larger for increasing shock amplitudes.

8.2. Shock tube

The next test case is the shock tube introduced by Toumi [3], and also studied in [2, 4, 24]. This shock tube activates the resonance fix described in Section 6, since $v_\mathrm{g}=0$ and $v_\ell=0$ at $t=0\,\mathrm{s}$. The parameter in this fix is taken to be $\varepsilon=10^{-3}\,\mathrm{m/s}$. The initial states are given

DOI: 10.1002/fld

Table III. Relative error in Rankine-Hugoniot conditions for the isolated wave test

Wave 1		Wave 2		Wave 3	
$\sigma = -366.83$		$\sigma = -4.9214$		$\sigma = 10.000068$	
u_1	4.5857×10^{-5}	u_1	1.7004×10^{-5}	u_1	0.0
u_2	4.5305×10^{-5}	u_2	2.1544×10^{-5}	u_2	6.7568×10^{-5}
u_3	4.5612×10^{-5}	u_3	1.1157×10^{-3}	u_3	2.8099×10^{-5}(abs.)
u_4	4.5356×10^{-5}	u_4	-4.3392×10^{-4}	u_4	6.6350×10^{-5}
u_5	4.5855×10^{-5}	u_5	1.6157×10^{-5}	u_5	1.7770×10^{-4}(abs.)
u_6	4.5168×10^{-5}	u_6	2.0390×10^{-5}	u_6	6.4933×10^{-5}
Wave 4		Wave 5		Wave 6	
$\sigma = 76.579$		$\sigma = 100.033$		$\sigma = 514.69$	
u_1	4.2484×10^{-4}	u_1	3.3333×10^{-5}	u_1	8.1034×10^{-5}
u_2	4.2487×10^{-4}	u_2	0.0	u_2	8.0726×10^{-5}
u_3	4.2675×10^{-4}	u_3	3.3307×10^{-5}	u_3	8.1191×10^{-5}
u_4	4.2411×10^{-4}	u_4	-5.8668×10^{-4}(abs.)	u_4	8.1009×10^{-5}
u_5	4.2477×10^{-4}	u_5	3.3282×10^{-5}	u_5	8.1091×10^{-5}
u_6	4.2505×10^{-4}	u_6	-6.0766×10^{-3}(abs.)	u_6	8.0694×10^{-5}

in Table IV. In the regularisation term (10), $\delta = 2$ was used. The results at $t = 0.06\,\mathrm{s}$ for different grid resolutions are presented in Figure 1. The result from the MUSCL-MUSTA scheme with 2 substeps and the minmod slope limiter, presented in [2], is used for the reference curves on a grid of 10,000 cells. The curve for the Roe scheme presented in this article, on the same grid, match the reference curves to plotting accuracy. For the lower resolutions, the plateau between the slow waves is not well resolved. A similar behaviour is observed with the MUSCL-MUSTA method, but it is more pronounced with the Roe method, especially for the liquid velocity. To understand where this overshoot comes from, we use the similarity property of the solution. The shock tube is run on a fine grid of 10,000 cells, with the minmod limiter. The liquid-velocity profiles at different time steps are plotted against the similarity parameter x/t on Figure 2. We can see that an oscillation appears for the wave at $x/t \approx 100\,\mathrm{m/s}$, but that the wave after all converges to the expected wave. This is due to the limiter with the Lax and Liu smoothness-measure definition (cf. Section 7) being more imprecise the larger the jump is. Using the original definition of the smoothness measure by LeVeque, the original oscillation is present but much smaller. Note, however, that the latter requires that the waves be ordered the same way in adjacent computational cells, and therefore cannot generally be used with the present system. It is a particular case that it works on this test case, where the velocities keep the same ordering during the simulation. The oscillation does not appear at all without wave limiter, as shown on Figure 3.

Table IV. Initial states for Toumi's shock tube

	Symbol (unit)	Left	Right
Gas vol. frac.	α_g $(-)$	0.25	0.10
Pressure	p (MPa)	20	10
Gas velocity	v_g (m/s)	0	0
Liq. velocity	v_ℓ (m/s)	0	0
Temperatures	T_g, T_ℓ (K)	308.15	308.15

8.3. Moving Gauss curve

The Roe schemes without and with flux limiters are expected to be first and second order, respectively, for smooth solutions. This test case consists in a smooth volume-fraction profile

DOI: 10.1002/fld

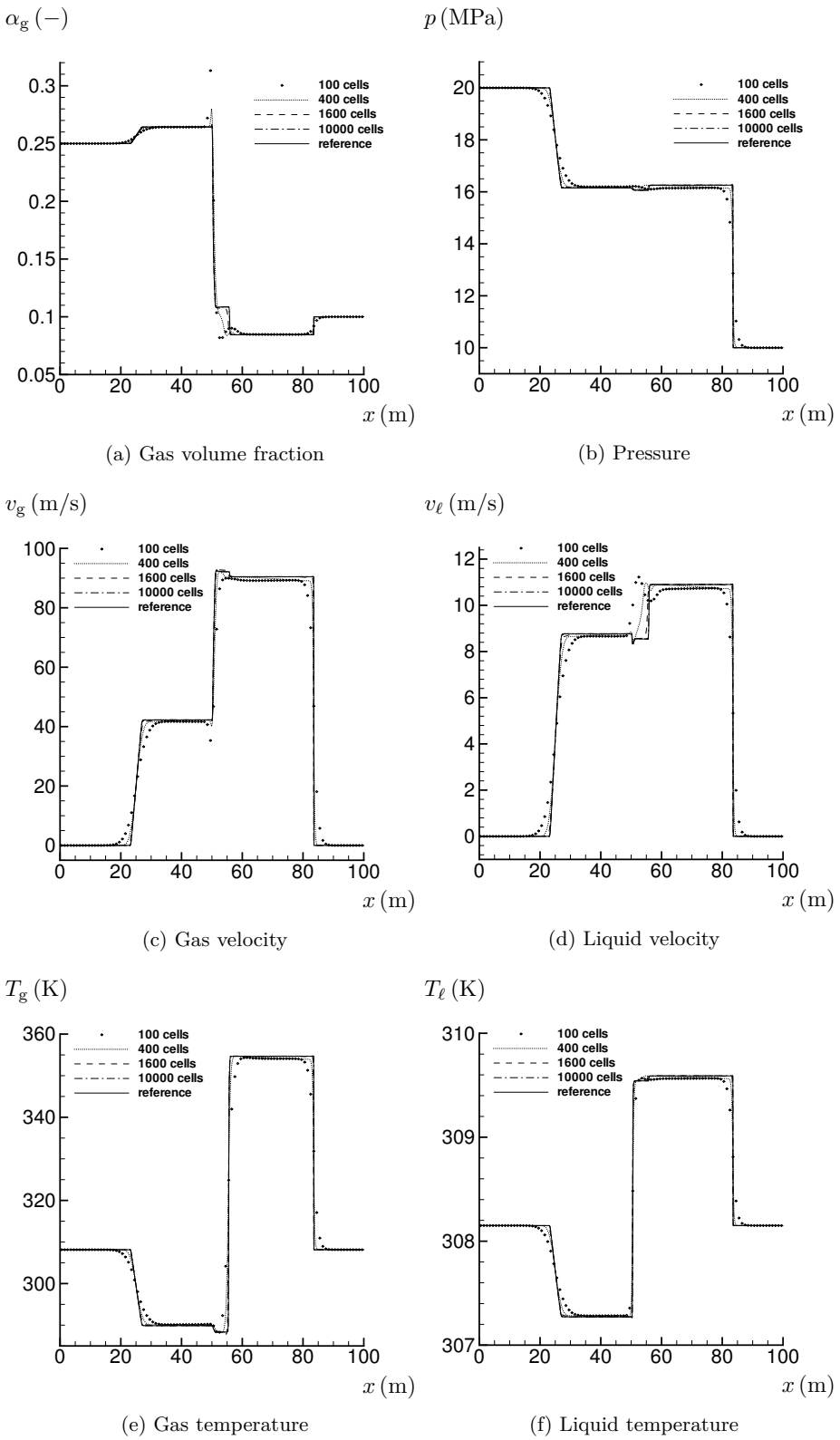

(a) Gas volume fraction

(b) Pressure

(c) Gas velocity

(d) Liquid velocity

(e) Gas temperature

(f) Liquid temperature

Figure 1. Convergence of the scheme with minmod limiter on Toumi's shock tube at $t = 0.06s$. CFL=0.5. The reference curves are produced with the MUSCL-MUSTA scheme, with the minmod slope limiter on a grid of 10,000 cells, CFL=0.5.

DOI: 10.1002/fld

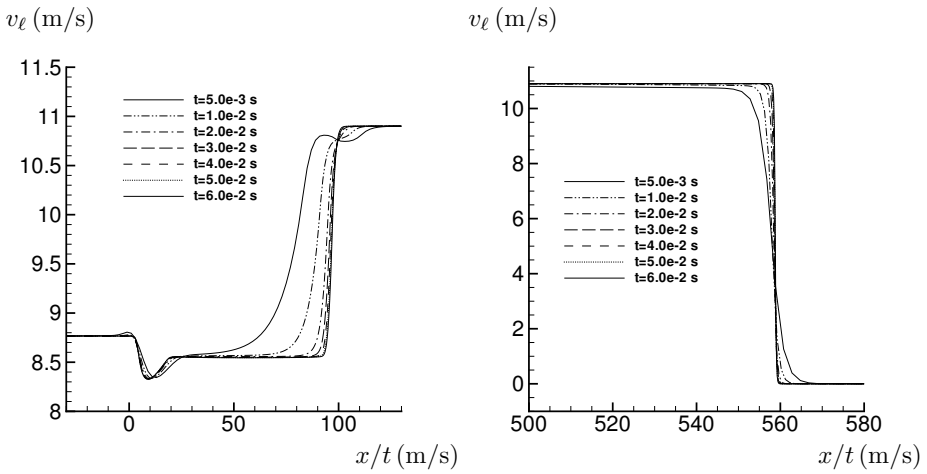

(a) Slow waves (b) Fast wave

Figure 2. Solution of Toumi's shock tube at different times plotted against the similarity parameter x/t. 10,000 cells, minmod limiter, CFL=0.5.

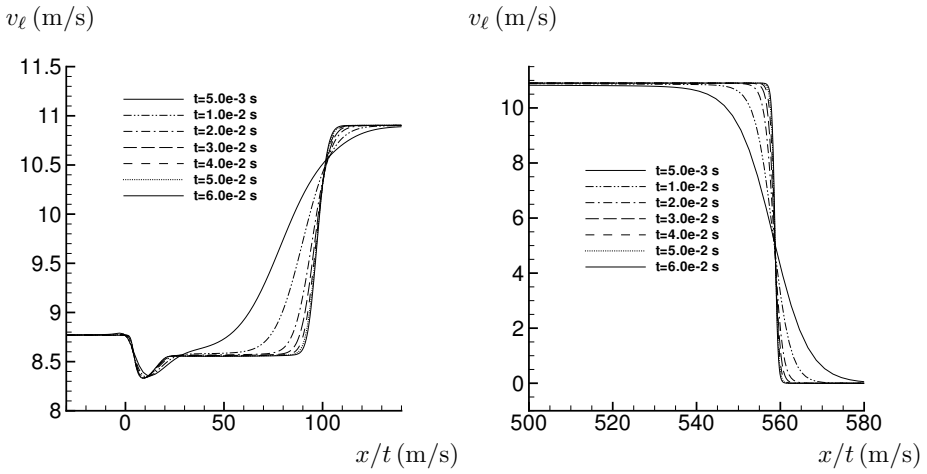

(a) Slow waves (b) Fast wave

Figure 3. Solution of Toumi's shock tube at different times plotted against the similarity parameter x/t. 10,000 cells, no limiter, CFL=0.5.

(a Gauss curve) being advected with the flow. The two phases having the same velocity, the profile should not be distorted. We use this case to evaluate the convergence order of the scheme.

The case is initialised with all the quantities being uniform, apart from the gas volume fraction which follows a scaled Gauss curve

$$\alpha_{\mathrm{g},0} = 0.1 + 0.8 \exp\left(-\frac{(x-\mu)^2}{2\sigma^2}\right) \tag{112}$$

where $\sigma = 0.42$ and $\mu = 6\,\mathrm{m}$. The other quantities are given in Table V.

The solution is compared to the analytical solution at $t = 0.03\,\mathrm{s}$. The Gauss curved is advected at the velocity 100 m/s, therefore the analytical solution is given by the equation (112) where σ is unchanged and $\mu = 9\,\mathrm{m}$. The error and the convergence order are listed in Table VI for the Roe scheme without wave limiter, and the Roe scheme with the minmod

DOI: 10.1002/fld

Table V. Initial state for the moving Gauss curve case

	Symbol (unit)	Initial value
Pressure	p (MPa)	0.1
Gas velocity	v_{g} (m/s)	100
Liq. velocity	v_{ℓ} (m/s)	100
Temperatures	$T_{\mathrm{g},\ell}$ (K)	315.9

wave limiter. The parameter in the resonance fix is $\varepsilon = 10^{-3}\,\mathrm{m/s}$. $\delta = 2$ was used in the regularisation term (10). Figure 4 gives an illustration of the convergence. We can see that for the scheme with wave limiter, the second order convergence is observed already from 200 cells. For the scheme without limiter, which is first order, the expected convergence order is attained for a finer grid than for the second order scheme.

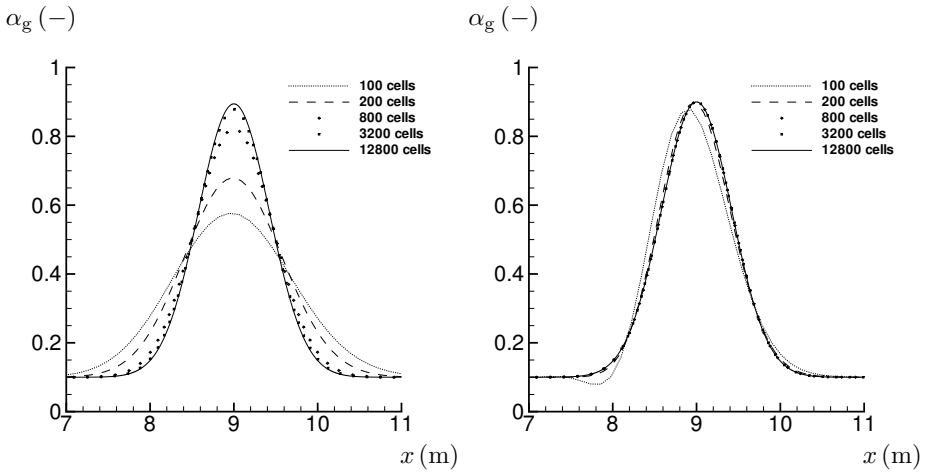

(a) No limiter (b) Minmod Limiter

Figure 4. Convergence for the moving Gauss curve, Roe with and without limiter. $t = 0.03s$.

Table VI. Moving Gauss curve: convergence order of the Roe scheme without wave limiter, and with the minmod wave limiter, both with a resonance fix parameter $\varepsilon = 10^{-3}\,\mathrm{m/s}$

	Roe		MC-Roe	
Cells	$\|\mathcal{E}(\alpha_{\mathrm{g}})\|_1$	n	$\|\mathcal{E}(\alpha_{\mathrm{g}})\|_1$	n
100	4.122×10^{-1}	–	1.192×10^{-1}	–
200	2.615×10^{-1}	0.66	3.028×10^{-2}	1.98
400	1.523×10^{-1}	0.78	7.625×10^{-3}	1.99
800	8.341×10^{-2}	0.87	1.908×10^{-3}	2.00
1600	4.386×10^{-2}	0.93	4.770×10^{-4}	2.00
3200	2.252×10^{-2}	0.96	1.193×10^{-4}	2.00
6400	1.142×10^{-2}	0.98	2.982×10^{-5}	2.00
12800	5.749×10^{-3}	0.99	7.455×10^{-6}	2.00

This test is also used to check the sensitivity of the solution to the parameter ε in the resonance fix. The velocities should remain uniform and equal to their initial value, but they are slightly deformed. Table VII shows the maximum error in the velocities as a function of ε. Recall that the ε parameter determines how close the gas and liquid velocities can be. We can see that the error is very dependent on it. In this test, it was not possible to decrease ε

DOI: 10.1002/fld

further. Otherwise, the code crashes due to the diagonalisation routine returning conjugate complex eigenvalues, though with negligible imaginary part. This is caused by a strong loss of numerical accuracy, since two eigenvectors become almost parallel. The matrix should in theory be diagonalisable with real eigenvalues. The ε parameter should be set so that the diagonalisation routine always returns real eigenvalues. A value of $\varepsilon = 10^{-3}\,\mathrm{m/s}$ worked well for this case.

Table VII. Moving Gauss curve: Maximum error in the gas and liquid velocities depending on the ε parameter in the resonance fix.

ε	$\|v_\mathrm{g} - 100\|_\mathrm{max}$	$\|v_\ell - 100\|_\mathrm{max}$
10^{-0}	8.35×10^{-2}	1.34×10^{-1}
10^{-1}	8.34×10^{-4}	1.30×10^{-3}
10^{-2}	8.34×10^{-6}	1.30×10^{-5}
10^{-3}	8.00×10^{-8}	1.30×10^{-7}

8.4. Water faucet

The last test is the water-faucet test case. It was introduced by Ransom [35] and is a standard test case for one-dimensional two-fluid models and numerical methods to solve them. In particular, it exposes the ability of the scheme to accurately capture the slow-moving mass waves, which is of interest e.g. in pipe-transport applications. This case has been studied for example in [2, 4, 9, 22, 24, 28, 36]. It consists in a vertical tube initially filled with a mixture of uniform gas fraction $\alpha_\mathrm{g} = 0.2$. The tube is closed for the gas at the top. The liquid flows downwards, and is injected from the top at a liquid fraction of $\alpha_\ell = 0.8$. At time $t = 0$, the gravity is turned on. The liquid already present in the tube accelerates downwards, while a thinning jet forms from the top of the tube. Some gas is sucked in in counter-current to fill the space freed by the thinning jet. Table VIII presents the parameters used in this work. $\delta = 1.2$ was used in the regularisation term (10).

Table VIII. Parameter values for the water-faucet test case

	Symbol (unit)	Value
Gas vol. frac.	α_g $(-)$	0.20
Pressure	p (MPa)	0.1
Gas velocity	v_g (m/s)	0.0
Liq. velocity	v_ℓ (m/s)	10.0
Temperatures	T_g, T_ℓ (K)	315.9
Gravity	g (m/s^2)	9.81

The upper boundary condition should impose a zero velocity on the gas phase, while allowing one characteristic to leave the domain, since the flow is subsonic and entering the tube. The four other characteristics are entering the domain. Therefore, five variables have to be set, while one is extrapolated. At the bottom, the liquid flows out at subsonic velocity, while the gas may flow in or out, at subsonic velocity. Depending on the gas velocity, three or four variables have to be extrapolated, while three or two respectively have to be set. Table IX shows the variables chosen (the same as in [2]), if they are extrapolated or set, and in the latter case, their value.

The entropy is evaluated according to the expression

$$s = C_p \ln\left(\frac{\gamma(p+p_\infty)^{\frac{1}{\gamma}}(p^0+p_\infty)^{1-\frac{1}{\gamma}}}{\rho(\gamma-1)C_pT^0}\right) \tag{113}$$

where T^0 and p^0 are some reference parameters at which $s = 0\,\mathrm{J/K}$. s_ℓ^in is once and for all evaluated with (113) at the initial pressure and temperature of the water jet (and using the

DOI: 10.1002/fld

Table IX. Variables for the boundary conditions for the water faucet case.

		Top		Bottom	
Variable	Unit		Value		Value
Volume fraction	$\alpha_\mathrm{g}\,(-)$	Set	0.2	Extrapolated	–
Pressure	$p\,(\mathrm{MPa})$	Extrapolated	–	Set	0.1
Momentum	$m_\mathrm{g}\,(\mathrm{kg}/(\mathrm{m}^2\cdot\mathrm{s}))$	Set	0	Extrapolated	–
Momentum	$m_\ell\,(\mathrm{kg}/(\mathrm{m}^2\cdot\mathrm{s}))$	Set	m_ℓ^in	Extrapolated	–
Entropy	$s_\mathrm{g}\,(\mathrm{J/K})$	Extrapolated	–	Set or Extr.	$s_\mathrm{g}^\mathrm{atm}$
Entropy	$s_\ell\,(\mathrm{J/K})$	Set	s_ℓ^in	Extrapolated	–

equation of state to evaluate the density), and remains the same over time. The momentum m_ℓ^in also remains constant over time, and is equal to the initial momentum of the water jet $m_\ell^{0,\mathrm{in}} = \rho_\ell^{0,\mathrm{in}} v_\ell^{0,\mathrm{in}}$ evaluated at the state given in Table VIII. Finally, in the case where the gas entropy has to be set at the bottom, $s_\mathrm{g}^\mathrm{atm}$ is equal to its initial value, evaluated using (113) and the values in Table VIII.

The results of a mesh sensitivity study are plotted at $t = 0.6s$ in Figure 5. They are compared to the results from the MUSCL-MUSTA scheme from [2], with the minmod slope limiter. This shows that the two schemes converge to the same solution, to plotting accuracy.

Finally, we assessed the computational efficiency of the Roe scheme compared to the MUSTA scheme. We compared the CPU time used to solve the water faucet case on grids from 50 to 800 cells, with the second order extension. Remark that the flux limiter approach for the Roe scheme requires a first-order forward Euler time step, while the MUSCL-MUSTA approach requires a second-order Runge-Kutta time step. The results are presented in Figure 6. In this case, the Roe and the MUSCL-MUSTA methods perform similarly in terms of convergence error compared to CPU time. However, the profiling of the code gives useful information. In the case of the Roe scheme, 60% of the CPU time is used on diagonalising the Jacobian, while only 3% is used on evaluating the primary variables, which means solving the equation of state. In the case of the MUSCL-MUSTA method with two substeps, 30% of the CPU time is used on solving the equation of state. Here, the stiffened gas equation of state is used, which is a simple one to solve. More accurate equations of state may take considerably more time to solve, thus impairing the efficiency of the MUSTA method.

9. CONCLUSION

A partially analytical Roe scheme for the six-equation two-fluid model has been derived and implemented. For most of the variables, an analytical Roe average is given. The average of the few remaining variables must generally be found numerically and is dependent on the equation of state. This makes the scheme flexible with respect to the choice of equation of state.

The central idea of this work was to include the non-conservative terms in the quasilinear form, so that the wave structure of the system reflects the effects of all the terms in the model. However, the numerical solution is dependent on the choice of an integration path for the non-conservative terms, which can present problems. One advantage of the present derivation is that the definition of the Roe averages can be made independent from the integration path. Only the averages of the non-conservative factors will be affected by a change of family of path.

We have seen that the six-equation two-fluid model with the regularisation used in this work is prone to resonance when the liquid and gas velocity are equal. The Jacobian matrix becomes non-diagonalisable. A fix has been devised by taking advantage of the continuity of the eigenvalues and eigenvectors.

DOI: 10.1002/fld

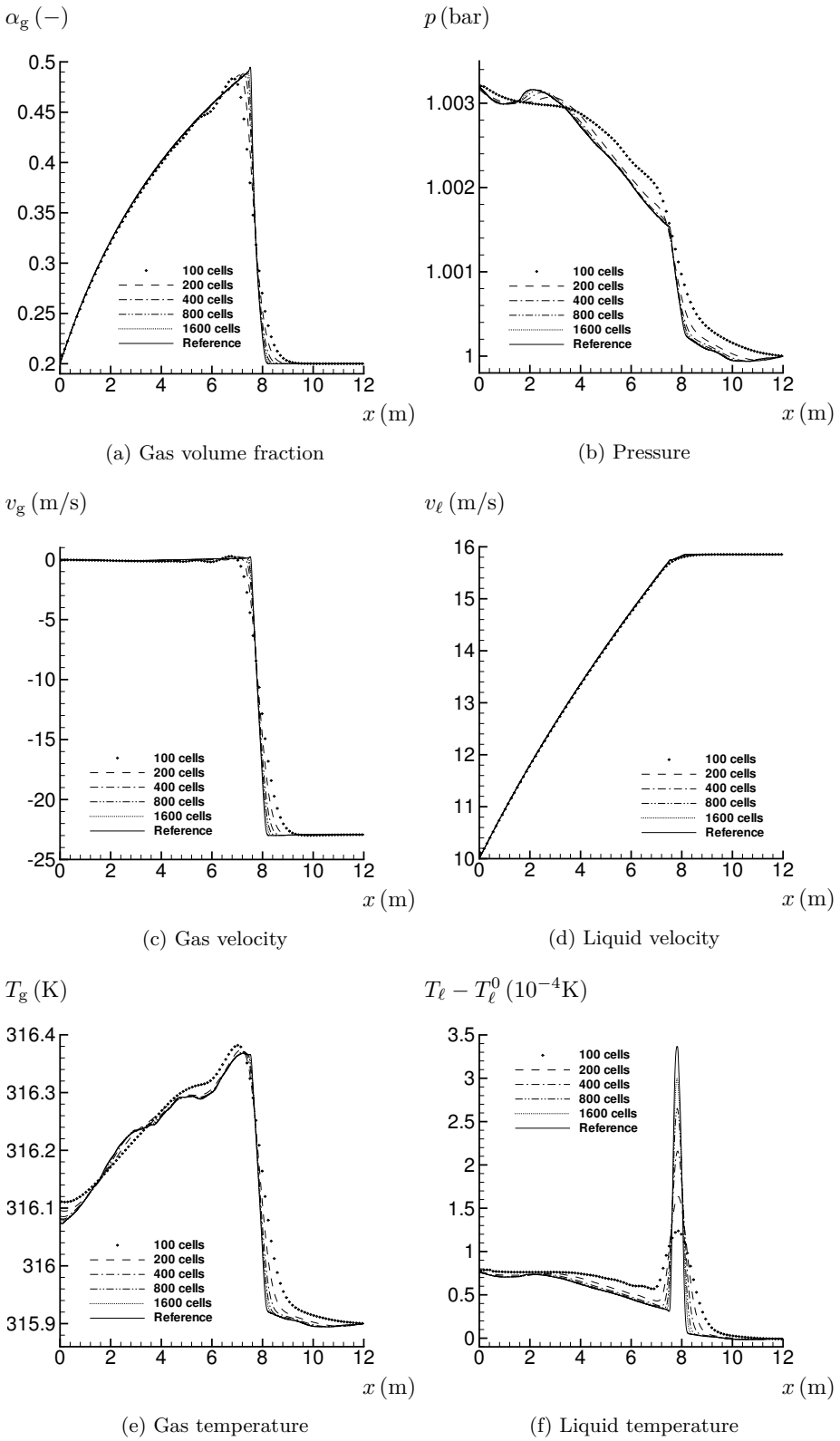

(a) Gas volume fraction

(b) Pressure

(c) Gas velocity

(d) Liquid velocity

(e) Gas temperature

(f) Liquid temperature

Figure 5. Convergence of the scheme on the water faucet test case at $t = 0.6s$ with the minmod wave limiter. CFL=0.5. The reference curves are produced with the MUSCL-MUSTA scheme, with the minmod slope limiter on a grid of 10,000 cells, CFL=0.5.

DOI: 10.1002/fld

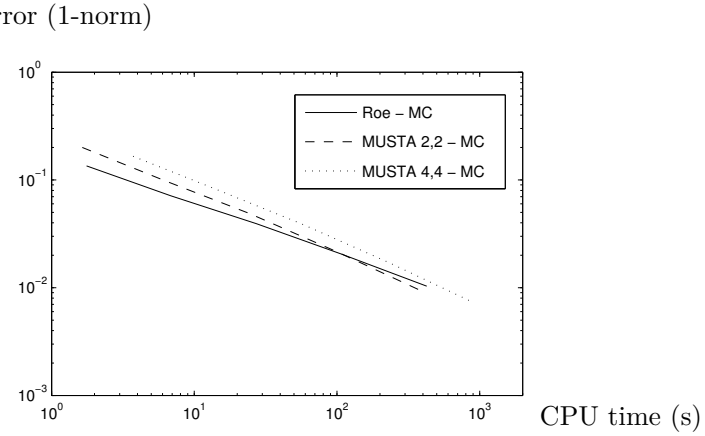

Figure 6. CPU time versus 1-norm of the error on α_g of the numerical solution compared to the reference (Roe scheme, MC limiter, 10000 cells). 50 to 800 cells, Roe and MUSCL-MUSTA with MC limiter, t=0.6s, CFL=0.5. Fortran 90 on an Intel® Xeon® CPU X5570 at 2.93GHz.

Finally, four test cases show that the scheme performs well. Even though some previous work showed that the *formally path-consistent* approach can feature a wrong wave structure, the test cases show that this problem is limited here.

A. ISOLATED WAVES

The common left state for the isolated wave test is given in Table X. The right states are found from $\Delta \boldsymbol{U}$ listed in Table XI through

$$\boldsymbol{U}_R = \boldsymbol{U}_L + \Delta \boldsymbol{U}. \tag{114}$$

Table X. Left state for the isolated wave test

	Symbol	Value
Gas vol. frac.	$\alpha_g\,(-)$	0.2
Pressure	$p\,(\mathrm{Pa})$	1×10^7
Gas density	$\rho_g\,(\mathrm{kg/m^3})$	100
Liq. density	$\rho_\ell\,(\mathrm{kg/m^3})$	1000
Gas. velocity	$v_g\,(\mathrm{m/s})$	100
Liq. velocity	$v_\ell\,(\mathrm{m/s})$	10

ACKNOWLEDGEMENT

A.M. and S.T.M. were financed through the BIGCCS Centre. T.F. was financed through the CO_2 Dynamics project. The authors acknowledge the support from the Research Council of Norway (189978, 193816), Aker Solutions, ConocoPhilips, Det Norske Veritas, Gassco, GDF SUEZ, Hydro, Shell, Statoil, TOTAL and Vattenfall.

References

1. Stewart HB, Wendroff B. Two-phase flow: Models and methods. *J. Comput. Phys.* 1984; **56** : 363–409.
2. Munkejord ST, Evje S, Flåtten T. A MUSTA scheme for a nonconservative two-fluid model. *SIAM J. Sci. Comput.* 2009; **31** : 2587–2622.

DOI: 10.1002/fld

Table XI. $\Delta \boldsymbol{U}$ for the isolated wave test

Wave 1		Wave 2		Wave 3	
α_{g}	-7.0948×10^{-5}	α_{g}	-7.5304×10^{-5}	α_{g}	0.0
p	1.3294×10^{4}	p	-6.6182×10	p	0.0
ρ_{g}	9.5032×10^{-2}	ρ_{g}	-2.0232×10^{-5}	ρ_{g}	0.0
ρ_{ℓ}	5.5275×10^{-3}	ρ_{ℓ}	1.5760×10^{-4}	ρ_{ℓ}	-1.3006
v_{g}	-2.7770×10^{-1}	v_{g}	3.9541×10^{-2}	v_{g}	0.0
v_{ℓ}	-3.5498×10^{-2}	v_{ℓ}	-1.4068×10^{-3}	v_{ℓ}	0.0
Wave 4		**Wave 5**		**Wave 6**	
α_{g}	7.5127×10^{-5}	α_{g}	0.0	α_{g}	6.6758×10^{-5}
p	-3.2942×10^{2}	p	0.0	p	-2.3681×10^{4}
ρ_{g}	-4.3715×10^{-3}	ρ_{g}	2.8360×10^{-1}	ρ_{g}	-1.6911×10^{-1}
ρ_{ℓ}	-9.5450×10^{-5}	ρ_{ℓ}	0.0	ρ_{ℓ}	-9.8297×10^{-3}
v_{g}	-7.7818×10^{-3}	v_{g}	0.0	v_{g}	-5.6380×10^{-1}
v_{ℓ}	-6.2563×10^{-3}	v_{ℓ}	0.0	v_{ℓ}	-4.7076×10^{-2}

3. Toumi I. An Upwind Numerical Method for Two-Fluid Two-Phase Flow Models. *Nuclear Science and Engineering* 1996; **123** : 147–168.
4. Paillère H, Corre C, García Cascales JR. On the extension of the AUSM^{+} scheme to compressible two-fluid models. *Comput. & Fluids* 2003; **32** : 891–916.
5. Bendiksen KH, Malnes D, Moe R, Nuland S. The dynamic two-fluid model OLGA: Theory and application. *SPE Prod. Eng.* 1991; **6** : 171–180.
6. Bestion D. The physical closure laws in the CATHARE code. *Nuclear Engineering and Design* 1990; **124** : 229–245.
7. Larsen M, Hustvedt E, Hedne P, Straume T. Petra: A novel computer code for simulation of slug flow. Proc. of *SPE Annual Technical Conference and Exhibition, SPE 38841* 1997; 1–12.
8. *WAHA3 Code Manual*, JSI Report IJS-DP-8841, Jožef Stefan Insitute, Ljubljana, Slovenia, 2004.
9. Coquel F, El Amine K, Godlewski E. A numerical method using upwind schemes for the resolution of two-phase flows. *J. Comput. Phys.* 1997; **136** : 272–288.
10. Parés C. Numerical Methods for Non-Conservative Hyperbolic Systems: A Theoretical Framework. *SIAM J. Numer. Anal.* 2006; **44** : 300–321.
11. Toro EF. Riemann solvers with evolved initial conditions. *Internat. J. Numer. Methods Fluids* 2006; **52** : 433–453.
12. Castro CE, Toro EF. A Riemann solver and upwind methods for a two-phase flow model in non-conservative form. *Internat. J. Numer. Methods Fluids* 2006; **50** : 275–307.
13. Martínez Ferrer PJ, Flåtten T, Munkejord ST. On the effect of temperature and velocity relaxation in two-phase flow models. *ESAIM: M2AN* 2012; **46** : 411–442.
14. Morin A, Flåtten T and Munkejord ST. Towards a formally path-consistent Roe scheme for the six-equation two-fluid model. *AIP Conference Proceedings* 2010; **1281** : 71–74.
15. Castro MJ, LeFloch PG, Muñoz-Ruiz ML, Parés C. Why many theories of shock waves are necessary: Convergence error in formally path-consistent schemes. *J. Comput. Phys.* 2008; **227** : 8107–8129.
16. Abgrall R, Karni S. A comment on the computation of non-conservative products. *J. Comput. Phys.* 2010; **229** : 2759–2763.
17. Toro EF. MUSTA: A multi-stage numerical flux. *Appl. Numer. Math* 2006; **56** : 1464–1479.
18. Toro EF, Titarev VA. MUSTA fluxes for systems of conservation laws. *J. Comput. Phys.* 2006; **216** : 403–429.
19. Roe PL. Approximate Riemann solvers, parameter vectors, and difference schemes. *J. Comput. Phys.* 1981; **43** : 357–372.
20. Lax PD. On the notion of hyperbolicity. *Comm. Pure Appl. Math.* 1980; **33** : 395–397.
21. Cortes J, Debussche A, Toumi I. A density perturbation method to study the eigenstructure of two-phase flow equation systems. *J. Comput. Phys.* 1998; **147** : 463–484.
22. Evje S, Flåtten T. Hybrid Flux-Splitting Schemes for a Common Two-Fluid Model. *J. Comput. Phys.* 2003; **192** : 175–210.
23. Chang CH, Liou MS. A robust and accurate approach to computing compressible multiphase flow: Stratified flow model and AUSM^{+}-up scheme. *J. Comput. Phys.* 2007; **225** : 850–873.
24. Munkejord ST. Comparison of Roe-type methods for solving the two-fluid model with and without pressure relaxation. *Comput. & Fluids* 2007; **36** : 1061–1080.
25. Stuhmiller JH. The influence of interfacial pressure forces on the character of two-phase flow model equations. *Int. J. Multiphas. Flow* 1977; **3** : 551–560.
26. Toumi I, Kumbaro A. An Approximate Linearized Riemann Solver for a Two-Fluid Model. *J. Comput. Phys* 1996; **124** : 286–300.
27. Toumi I. A Weak Formulation of Roe's Approximate Riemann Solver. *J. Comput. Phys.* 1992; **102** : 360–373.

DOI: 10.1002/fld

28. Muñoz-Ruiz ML, Parés C. Godunov Method for Nonconservative Hypebolic Systems. *ESAIM: M2AN* 2007; **41** : 169–185.
29. Morin A, Aursand PK, Flåtten T, Munkejord ST. Numerical Resolution of CO_2 Transport Dynamics. Proc. of *SIAM Conference on Mathematics for Industry: Challenges and Frontiers (MI09)*, San Francisco, CA, USA, October 9–10, 2009.
30. Flåtten T, Morin A, Munkejord ST. On solutions to equilibrium problems for systems of stiffened gases. *SIAM Journal on Applied Mathematics* 2011; **71** : 41–67.
31. LeVeque RJ. *Finite Volume Methods for Hyperbolic Problems*, Cambridge University Press 2002, ISBN 0-521-00924-3.
32. Soo SL. *Multiphase fluid dynamics*. Science Press, Beijing 1990, ISBN 0–291–39781–6.
33. van Leer B. Towards the ultimate conservative difference scheme V. A second order sequel to Godunov's method. *J. Comput. Phys.* 1979; **32** : 101–136.
34. Lax PD, Liu XD. Solution of two dimensional Riemann problem of gas dynamics by positive schemes. *SIAM J. Sci. Comput.* 1998; **19** : 319–340.
35. Ransom VH. Faucet flow. *Numerical Benchmark Tests, Multiphase Science and Technology, Vol. 3*, G. F. Hewitt, J. M. Delhaye and N. Zuber eds. Hemisphere/Springer, Washington DC, 1987, 465–467.
36. Trapp JA, Riemke RA. A nearly-implicit hydrodynamic numerical scheme for two-phase flows. *J. Comput. Phys.* 1986; **66** : 62–82.

DOI: 10.1002/fld